Informes Técnicos Ciemat

1279

Febrero, 2013

Current Travertines Precipitation from CO_2-rich Groundwaters as an Alert of CO_2 Leakages from a Natural CO_2 Storage at Gañuelas-Mazarrón Tertiary Basin (Murcia, Spain)

J. Rodrigo-Naharro
A. Delgado
M. J. Herrero
A. Granados
L. Pérez del Villar

GOBIERNO DE ESPAÑA
MINISTERIO DE ECONOMÍA Y COMPETITIVIDAD
Ciemat
Centro de Investigaciones Energéticas, Medioambientales y Tecnológicas

Informes Técnicos Ciemat

1279

Febrero, 2013

Current Travertines Precipitation from CO_2-rich Groundwaters as an Alert of CO_2 Leakages from a Natural CO_2 Storage at Gañuelas-Mazarrón Tertiary Basin (Murcia, Spain)

J. Rodrigo-Naharro
A. Delgado[1]
M. J. Herrero[2]
A. Granados[1]
L. Pérez del Villar

[1] *Instituto Andaluz de Ciencias de la Tierra (CSIC-URG)*

[2] *Dpto. de Petrología, Facultad de Ciencias Geológicas (UCM)*

Departamento de Medio Ambiente

Toda correspondencia en relación con este trabajo debe dirigirse al Servicio de Información y Documentación, Centro de Investigaciones Energéticas, Medioambientales y Tecnológicas, Ciudad Universitaria, 28040-MADRID, ESPAÑA.

Las solicitudes de ejemplares deben dirigirse a este mismo Servicio.

Los descriptores se han seleccionado del Thesauro del DOE para describir las materias que contiene este informe con vistas a su recuperación. La catalogación se ha hecho utilizando el documento DOE/TIC-4602 (Rev. 1) Descriptive Cataloguing On-Line, y la clasificación de acuerdo con el documento DOE/TIC.4584-R7 Subject Categories and Scope publicados por el Office of Scientific and Technical Information del Departamento de Energía de los Estados Unidos.

Catálogo general de publicaciones oficiales
http://www.060.es

Depósito Legal: M -26385-2011
ISSN: 1135 - 9420
NIPO: 721-13-013-8

Editorial CIEMAT

CLASIFICACIÓN DOE Y DESCRIPTORES

S54
TRAVERTINE; CALCITE; ARAGONITE; CARBON DIOXIDE; STABLE ISOTOPES; NATURAL ANALOGUE; GREENHOUSE GASES

Current Travertines Precipitation from CO_2-rich Groundwaters as an alert of CO_2 Leakages from a Natural CO_2 Storage at Gañuelas-Mazarrón Tertiary Basin (Murcia, Spain)

Rodrigo-Naharro, J.; Delgado, A.; Herrero, M. J.; Granados, A.; Pérez del Villar, L.

54 pp. 19 figs. 101 refs. 7 tables

Abstract:

Carbon capture and storage technologies (CCS) represent the most suitable solutions related to the high anthropogenic CO_2 emissions to the atmosphere. As a consequence, monitoring of the possible CO_2 leakages from an artificial deep geological CO_2 storage (DGS) is indispensable to guarantee its safety. Fast surficial travertine precipitation related to these CO_2 leakages can be used as an alert for these escapes. Since few studies exist focusing on the long-term behaviour of an artificial CO_2 DGS, natural CO_2 storage affected by natural or artificial escapes must be studied as natural analogues for predicting the long-term behaviour of an artificial CO_2 storage. In this context, a natural CO_2 reservoir affected by artificial CO_2 escapes has been studied in this work. This study has mainly focused on the current travertines precipitation associated with the upwelling CO_2-rich waters from several hydrogeological wells drilled in the Gañuelas-Mazarrón Tertiary basin (SE Spain), and consists of a comprehensive characterisation of parent-waters and their associated carbonates, including elemental and isotopic geochemistry, mineralogy and petrography.

Geochemical characterisation of groundwaters has led to recognise 4 hydrofacies from 3 different aquifers. These groundwaters have very high salinity and electrical conductivity; are slightly acid; present high dissolved inorganic carbon (DIC) and free CO_2; are oversaturated in both aragonite and calcite; and dissolve, mobilize and transport low quantities of heavy and/or toxic elements. Isotopic values indicate that: i) the origin of parent-waters is related to rainfalls from clouds originated in the Mediterranean Sea or continental areas; ii) the origin of C is mainly inorganic; and iii) sulphate anions come mainly from the dissolution of the Messinian gypsum from the Tertiary Basin sediments.

Current travertines precipitation seems to be controlled by a combination of several factors, such as: i) a fast decrease of the hydrostatic pressure and the pCO_2, resulting in a rapid degassing process; and ii) microbes and algae activity. This process leads to an increase in pH that favours the carbonates precipitation. Although there are not master physicochemical parameters controlling the precipitation of calcite or aragonite from their respective parent-waters, it is suggested that some parent-waters have the most suitable physicochemical features for the precipitation of one or another polymorph. Finally, the $\delta^{13}C$ values of DIC and carbonates could be used as good tracers for CO_2 leakages from an artificial CO_2 DGS.

Precipitación Actual de Travertinos a Partir de Aguas Ricas en CO_2 como una Alerta de Escapes de CO_2 a Partir de un Almacenamiento Natural de CO_2 en la Cuenca Terciaria de Gañuelas-Mazarrón (Murcia, España)

Rodrigo-Naharro, J.; Delgado, A.; Herrero, M. J.; Granados, A.; Pérez del Villar, L.

54 pp. 19 figs. 101 refs. 7 tablas

Resumen:

Las tecnologías de Captura y Almacenamiento de CO_2 (CAC) representan la solución más adecuada a las emisiones antropogénicas de CO_2 a la atmósfera. En consecuencia, la monitorización de las posibles fugas de CO_2 de un almacenamiento geológico profundo (AGP) artificial de CO_2 es indispensable para garantizar su seguridad. La precipitación rápida y superficial de travertinos relacionada con estas fugas de CO_2 puede utilizarse como señal o alerta de dichos escapes. Dado que existen pocos estudios sobre el comportamiento, a largo plazo, de un AGP de CO_2 artificial, los almacenamientos naturales de este gas, afectados por escapes naturales o artificiales, deben ser estudiados como análogos naturales de un AGP de CO_2 para predecir su comportamiento a largo plazo. En este contexto se ha estudiado, en la Cuenca Terciaria de Ganuelas-Mazarrón (Murcia), un almacenamiento natural de CO_2 perturbado por sondeos hidrogeológicos, que permiten el escape de dicho CO_2 natural. Este estudio se ha centrado en los travertinos que están precipitando en relación con las aguas ricas en carbono inorgánico disuelto (DIC) de algunos de dichos sondeos. Dicho estudio ha consistido en la caracterización exhaustiva de dichos travertinos, así como de sus aguas madre, incluyendo la geoquímica elemental e isotópica, la mineralogía y la petrografía de dichas rocas.

La caracterización hidrogeoquímica de las aguas subterráneas ha permitido reconocer 4 hidrofacies pertenecientes a 3 acuíferos distintos. Dichas aguas tienen una salinidad y conductividad eléctrica muy altas; son ligeramente ácidas; presentan un alto contenido en DIC y CO_2 libre; están sobresaturadas en aragonito y calcita; y disuelven, movilizan y transportan escasas cantidades de elementos pesados y/o tóxicos. Los valores isotópicos indican que: i) el origen de las aguas madre está relacionado con las aguas de lluvias de nubes originadas en el mar Mediterráneo o en áreas continentales; ii) el origen del C es principalmente inorgánico; y iii) los sulfatos proceden principalmente de la disolución del yeso Messiniense existente en los sedimentos terciarios que rellenan la cuenca.

La precipitación actual de travertinos parece estar controlada por una combinación de varios factores, tales como: i) la disminución rápida de la presión hidrostática y la pCO_2, que provoca un proceso rápido de desgasificación; y ii) la actividad biológica en el medio. Este proceso conduce a un aumento en el pH del agua favoreciendo la precipitación rápida de los carbonatos. A pesar de que en las respectivas aguas madre no se han observado parámetros fisicoquímicos concluyentes para el control de la precipitación de calcita o aragonito, se sugiere que algunas aguas madre presentan las características fisicoquímicas más adecuadas para la precipitación de uno u otro polimorfo. Por último, los valores $\delta^{13}C$ del DIC y de los carbonatos de estos travertinos podrían ser utilizados como buenos trazadores para las fugas de CO_2 de un AGP artificial de este gas.

ACKNOWLEDGEMENTS

This work was carried out in the framework of a Singular Strategic Project (PSE-120000-2008-6) devoted to the CCS technologies, specifically in the sub-project PSS-120000-2008-31, focused on the CO_2 geological storage. This project was supported by the Spanish Ministry of Science and Innovation and EU FEDER funds. The authors acknowledge Mr. Miguel Ángel Labajo (CIEMAT) for the SEM analyses; Mr. Luis Gutiérrez and Ms. Marta Pelayo (CIEMAT) for the XRD analyses.

INDEX

1. INTRODUCTION

Current continental carbonates precipitation are related to pedogenic (soils, palaeosoils, calcretes); lacustrine and palustrine; karst caves (speleothems), and hot and cold springs, that result in travertine and tufa deposits. The travertines and tufas precipitating from the **s**prings are the result of the physical degassing and/or biochemical CO_2 consumption along streams and pools (Guo and Riding, 1998; Herrero and Escavy, 2010). Travertines often precipitate together with cyanobacteria, bacteria, algae, mosses and plants (Pentecost, 1990; Guo and Riding, 1998; 1999). Their classification is mainly based on two variables: water temperature and geological source of the spring water (Ford and Pedley, 1996; Jones and Renault, 2010). Based on the first variable, travertines are classified as cool (<20 ºC) and thermal (>20 ºC), the latter being in turn subdivided into warm (20-40 ºC), mesothermal (40-75 ºC) and hyperthermal (>75 ºC) (Pentecost, 2005). However, according to Pentecost and Viles (1994), Pentecost (2005) and Viles and Pentecost (2007) springs are divided according to their water source in: i) metogene, with low DIC, low mineral depositional rates, relative low water T and depleted in ^{13}C, with more frequent $\delta^{13}C$ values between -3 to -12‰; and ii) thermogene, with higher pCO_2 than in soils, relatively hot water, rapid CO_2 degassing and high depositional rates, and with $\delta^{13}C$ values generally between -3 and 11‰ (Pentecost, 2005).

Travertine forms where groundwaters erupt to the surface, cool down, degass and, as a result, carbonate minerals precipitate. These minerals are normally aragonite, calcite and more rarely dolomite, with a variety of crystal morphologies and chemical compositions. Numerous studies (Moore, 1956; Friedman, 1970; Folk, 1974, 1994; Pentecost and Viles, 1994; Farmer and Des Marais, 1994; Ford and Pedley, 1996; Guo and Riding, 1998, 1999; Frisia et al., 2000; Pentecost, 2005; Viles and Pentecost, 2007; Jones and Renault, 2010) tried to establish the master variables controlling the precipitation of one or another phase. These variables include temperature; growing inhibitors; water saturation index with respect to $CaCO_3$; CO_2 degassing rates and/or evaporation with the consequent decrease in pH; and the influence of plants, algae and bacterial activity (photosynthesis/respiration). Since aragonite travertines have a very metastable mineralogical composition, these rocks can undergo intensive diagenetic processes, even soon after precipitation (Guo et al., 1996), generally toward low Mg-calcite. In the context of a natural analogue of artificial storage of CO_2, the fast

travertines precipitation can be considered as a clear evidence of CO_2 leakages from groundwaters contaminated by CO_2, previously injected into a suitable geological formation, likely deep saline aquifers. The comprehensive study of deep CO_2-rich natural systems or natural analogues of CO_2 storage and leakage, including current travertines formation as a natural alarm of CO_2 escapes, is a very powerful tool to understand the mechanisms controlling the sealing effectiveness of an artificial CO_2 storage (Prado-Pérez, 2011; Prado-Pérez and Pérez del Villar, 2011; Prado-Pérez et al., 2012).

In the framework of a large project focused on the Carbon Capture and Storage (CCS) technologies, particularly on the Spanish CO_2 storage and leakage natural analogues (PSE-120000-2008-6; SubProject PSS-120000-2008-31), the Gañuelas-Mazarrón Tertiary Basin (Province of Murcia), hosting a CO_2-enriched deep saline aquifer is being studied (Pérez del Villar et al., 2009; Nisi et al., 2010a, 2010b; Rodrigo-Naharro et al., 2011, 2012, 2013). In this basin, numerous hydrogeological wells were drilled during 1960s for agricultural purposes. Besides this, two deep wells for geothermal exploration were also performed during 1980s, intersecting the abovementioned aquifer, being artesian wells currently (Rodríguez-Estrella, 2006). The deep CO_2-rich saline aquifer is hosted in an extensive and sometimes very thick marble formation, being the cap-rock a Tertiary marls formation (>500 m thick) that avoids CO_2 leakages. This sealing formation was effective until the over-exploitation of the shallowest fresh aquifers, causing their contamination by the deep-seated CO_2 (Cerón et al., 1998, 2000). In addition, free CO_2 is escaping to the atmosphere from the two aforementioned geothermal wells, known as El Saladillo and El Reventón.

Fast travertines precipitation occur in relation to groundwaters emerging from some of these hydrogeological and geothermal wells, being these carbonates the main object of this work, with the following aims: i) to establish the interplay of water chemistry, physical processes, hydrology and biotic activity responsible for their precipitation; ii) to correlate the different spring water chemistry with changes in the fabric and composition of the travertines; and iii) to discuss and determine the physicochemical and biological master variables controlling the precipitation of calcite, aragonite or both. In order to achieve these objectives, a comprehensive study of the emerging groundwaters from five wells, including physicochemical and isotopic features; and the travertine formations, including mineralogical, petrographic, geochemical and isotopic characteristics, has been performed. Data obtained from this research have also allowed

to consider the natural system studied as an excellent example of a natural analogue of CO_2 storage anthropogenically perturbed, with relevant CO_2 escapes.

2. GEOLOGICAL BACKGROUND

The Gañuelas-Mazarrón Tertiary basin is located in the SE of the Iberian Peninsula, inside the Internal Zones of the Betic Cordillera, in the transition between the Central and Oriental zones; specifically delimited by the so-called Águilas Arch, and Cartagena and Moreras Mountains (Fig. 1). This basin can be considered as a little sub-basin tectonically related to the Guadalentín Tertiary basin.

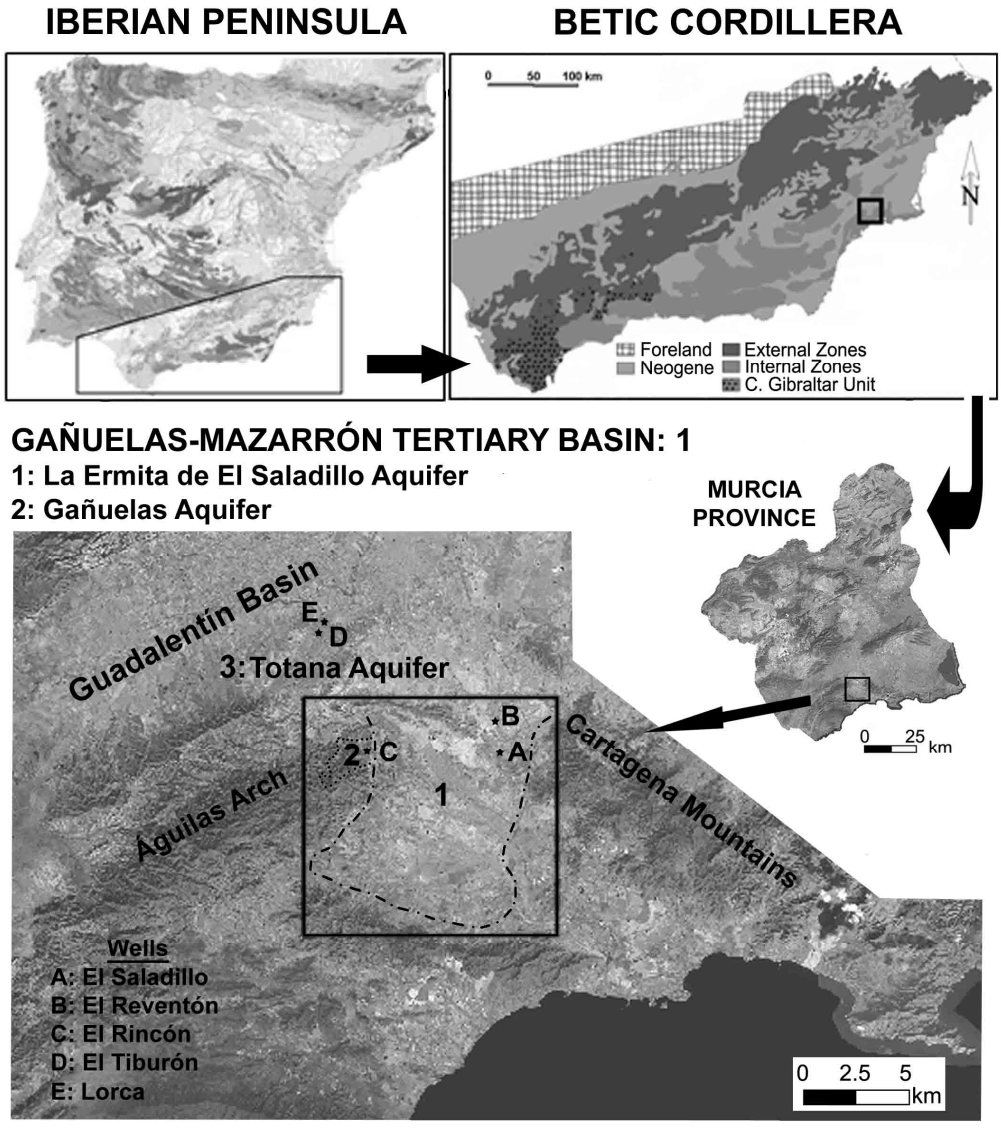

Fig. 1. Geographical and geological location of the Gañuelas-Mazarrón Tertiary basin, and the hydrogeological and geothermal wells intersecting the aquifers studied. Notice that the area of the La Ermita de El Saladillo aquifer (1) and the Gañuelas-Mazarrón Tertiary basin (1) approximately coincide.

At a smaller scale, the studied sub-basin is constituted of a thick Neogene sedimentary formation that unconformably overlays a Permo-Triassic metamorphic basement, composed of the Nevado Filábride, Alpujárride and Maláguide Complexes. The former, mainly consisting of schists, quartzites, gneisses, marbles and limestones bearing gypsum, belongs to the Permo-Triassic. The second Complex comprises schists, slates, quartzites, salts, conglomerates and sandstones of Paleozoic age, as well as Triassic limestones and dolomite rocks. The Maláguide Complex, not clearly represented in the studied zone, is constituted of Permo-Triassic sandstones, quartzites, slates and limestones (Cerón et al. 1998, 2000). Almost all of these geological materials are represented in the abovementioned reliefs delimiting the Gañuelas-Mazarrón Tertiary basin, which is filled by a sedimentary succession of conglomerates, calc-marls, with more or less gypsum, limestones, sandstones and calc-sandstones. These materials were intruded by Miocene andesites, dacites and rhyodacites, particularly in the faulted boundaries of the basin (IGME, 1974; Barragán, 1997). The Neogene deposits are in turn covered by Plio-Quaternary conglomerates, sands, silts and argillites.

It is noticeable that this basin is located in a currently very active seismic region, where earthquakes have traditionally been related to the main fault systems in the area (IGME, 1985; Sanz de Galdeano et al., 1995). Recently, the Lorca earthquake (2011) has been explained as caused by crustal unloading stresses at the upper frictional transition of the seismogenic layer, induced by groundwaters extraction (González et al., 2012). In this sense, according to Cerón et al. (1998, 2000), the Gañuelas-Mazarrón and Guadalentín basins are characterised by the presence of numerous hydrogeological wells performed in the 1960s for agricultural purposes. This continuous groundwaters over-exploitation originated a consequent drop of the water table and pressure, causing the uprising of deep saline CO_2-rich groundwaters.

Hydrogeologically, mainly five different aquifers were recognised in the Gañuelas-Mazarrón basin and its surrounding mountains (IGME, 1981): La Ermita de El Saladillo, Gañuelas, La Majada, La Majada-Leyva and Las Moreras. Among them, the La Ermita de El Saladillo and Gañuelas aquifers are the most interesting for the aims of this research work. In addition, the Totana aquifer, located to the NW, but in the boundary between the Gañuelas-Mazarrón and Guadalentin basins, is also interesting because their groundwaters originate travertines with similar features to those from the La Ermita de El Saladillo and Gañuelas groundwaters.

The La Ermita de El Saladillo aquifer, hosted in the Nevado-Filábride marble formation and Neogene volcanic rocks, has approximately 46 km^2. Tectonically is a graben delimited by extensional faults filled with volcanic rocks. This confined aquifer was intersected at 535 m (El Saladillo well) and 710 m depths (El Reventón well), both being artesian wells erupting high saline, acid and thermal waters (T~46 ºC). Besides this, the main feature of these groundwaters is the high concentration of DIC and free CO_2. Based on the R/Ra value (0.71), where R is the measured $^3He/^4He$ ratio and Ra is that of the air, i.e. $1.39x10^{-6}$, the contribution of mantle CO_2 was between 0 and 11%, considering an R/Ra average of 6.5 for European mantle. On the other part, the $\delta^{13}C_{(V-PDB)}$ of free CO_2 (-10.14‰) indicate that the CO_2 accumulation in the saline aquifer seems to be a mixture of two components: i) a CO_2 generated by thermometamorphic processes, affecting deep carbonate formations; and ii) a surficial/biogenic CO_2 (respiration), with a possible contribution of atmospheric CO_2 (R/Ra~1 for $^3He/^4He$ ratios) or, as has been mentioned, a small contribution of deep-seated CO_2 of likely mantle origin (Vaselli et al., 2010; Rodrigo-Naharro et al., 2011; 2012, 2013). In this sense, in the Cofrentes area, located 140 km towards NE, the R/Ra value (0.95) of free CO_2 also indicates a small contribution (~12%) of deep-seated CO_2 of likely mantle origin (Pérez et al., 1996; Cerón et al., 2000).

The Gañuelas aquifer has approximately 4 km^2 and it is also emplaced in the abovementioned marble formation. Tectonically is characterised by a series of recumbent folds towards the E. The central part of this aquifer is faulted, originating a structure in blocks. The basal Permo-Triassic schists from the Alpujárride Complex act as the impermeable formation. Finally, the Totana aquifer, of approximately 120 km^2, is hosted in lenticular detrital layers, more or less hydraulically connected among them, and intercalated in the Tertiary marly formation, filling the Guadalentín basin. This aquifer is very contaminated by the free CO_2 from the La Ermita de El Saladillo deep saline CO_2-rich aquifer. The main features of these aquifers are listed in Table 1, and their location is shown in Fig. 1.

Table 1
Main features of the aquifers located in the Gañuelas-Mazarrón Tertiary basin (IGME, 1979; Navarro et al., 1993).

Aquifer	Area (km^2)	Host rock lithology	Thickness (m)	Host lithology age	Water table depth (m)
La Ermita de El Saladillo	46	Marbles + Volcanic Rocks	60-90	Triassic + Miocene	460-550
Gañuelas	4	Marbles	200	Triassic	80
Totana	120	Detrital Sediments	Variable	Tertiary	150-250

3. MATERIALS AND METHODS

In order to accomplish the proposed objectives, both waters and the resulting carbonates were comprehensively studied from a hydrochemical, geochemical, petrographic and isotopic points of view. For these reasons, the methodology is extensively treated in this section, since we consider that it can be of great interest to evaluate the data reported in this work.

3. 1. Water samples

A total of 60 groundwater samples were taken during two field campaigns on September 2009 and March 2010. These samples are distributed as follows: 9 samples from the La Ermita de El Saladillo aquifer (El Saladillo and El Reventón wells); 28 from the Gañuelas aquifer (El Rincón well); and 23 from the Totana aquifer (El Tiburón and Lorca wells). All samples were stored at 4 °C before their analyses.

Two plastic vials, pre-washed with dilute HCl for 12 h and afterwards rinsed three times with distilled water, were taken for each water sample, which consisted of a chemically untreated aliquot of approximately 1 L for anion analyses. Another aliquot of approximately 100 mL, filtered through 0.1 μm filter and acidified with 65% ultra-pure HNO_3 to a pH <1, was used for cation determination. The pH values of natural waters were measured *in situ* by using a pH-metre, consisting of a voltmeter, a pH electrode and a temperature probe, with automatic compensation and accuracy better than 0.1 °C. It was calibrated by recording the electrical signal obtained by measuring the pH of two standard solutions, buffered to pH 4 and 7 at temperatures between 25

and 35 °C, similar to those of the samples. The electrical conductivity (EC) was measured *in situ* by a conductivity-metre with a K=1 cell and automatic temperature compensation in the range between 10 and 70 °C. In addition, *in situ* total alkalinity in each sample was also determined following the standard UNE-EN ISO 9963-1 and the method 2320, which is conveniently described in "Standard Methods for the Examination of Water and Wastewater". It is noticeable that under the hydrochemical conditions of the studied system, total and carbonate alkalinities were considered as equivalent.

Anion determinations were made in the geochemistry laboratories of the University of Zaragoza, almost immediately after sampling. The Cl^- content was determined by direct potentiometric measurement, by using an ORION 710-A potentiometre, equipped with automatic temperature compensation, and incorporating an Orion 94-17BN Cl^- specific electrode, and an ORION 90-0200 reference electrode. The same technique was used for F^- determination, but using an ORION94-09BN F^- selective electrode. Total dissolved SO_4^{2-} was indirectly determined by molecular absorption spectrometry, according to the Nemeth (1963) method. The PO_4^{3-} determinations were performed by means of a spectrophotometre at 420 nm, using the same equipment than for the measurements of total dissolved SO_4^{2-}.

Cation analyses (Ca, Na, Mg, K, Fe and Mn) were performed by using Atomic Absorption Spectrometry (AAS), while Al_2O_3 and SiO_2 were measured by Graphite Furnace Atomic Absorption Spectrometry (GFAAS) and Inductively Coupled Plasma-Optical Emission (ICP-OES), respectively. Trace elements (Sr, Be, Sc, V, Cr, Mn, Co, Ni, Cu, Zn, As, Se, Y, Mo, Cd, In, Sn, Sb, Ba, Au, Tl, Pb , Bi, Th, U, Li, B) were determined by Inductively Coupled Plasma-Mass Spectrometry (ICP-MS). These determinations were performed in the chemical laboratories of CIEMAT.

The analyses quality was guaranteed by the blanks, duplicates and multielemental patterns analyses made each ten samples, obtaining reproducible results within an error range between 3 and 5%. The charge balance calculation for each sample, by using the PHREEQC code (Parkhurst and Appelo, 1999) and WATEQ4F thermodynamic database (Ball and Nordstrom, 2001), was another analyses quality test. In this sense, charge balance error, as calculated by PHREEQC, generally was less than 5%, except for the El Saladillo water.

For the classification of water samples, Piper-Hill diagrams, obtained by means of the INAQUAS code (IGME, 2008), were used. Speciation-solubility calculations were performed by using the PHREEQC code and WATEQ4F thermodynamic database.

Isotope measurements were carried out at the Stable Isotope Biogeochemistry Laboratory of the Instituto Andaluz de Ciencias de la Tierra (CSIC-UGR, Granada). For the isotopic characterisation of water samples, the $\delta^{18}O$, $\delta^{2}H$, $\delta^{13}C_{(DIC)}$, and $\delta^{34}S$ and $\delta^{18}O$ of dissolved SO_4^{2-} were measured. Water oxygen was analyzed by using a modification of the CO_2-H_2O equilibration method (Cohn and Urey, 1938; Epstein and Mayeda, 1953). This method consists of equilibrating CO_2-H_2O at a constant temperature (25 ºC) in the presence of He. In order to measure the $^{18}O/^{16}O$ ratio, 5 aliquots of this equilibrated CO_2 are separated from other gases (small contaminations) by a chromatography column (GasBench II system, Thermo-Finnigan). Finally the isotopic ratio was analyzed in a Delta Plus XP mass spectrometer (Thermo). For the analysis of δD, an aliquot of water (0.5 μL) was injected into a ceramic column containing a glassy carbon tube at 1450 ºC, producing H_2 and CO gases (Sharp et al., 2001). The H_2 was separated by chromatography using a He carrier stream connected online with a Pyrolisis Furnace TC/EA (Thermo-Finnigan, Bremen, Germany) and analysed in a Delta Plus XL mass spectrometer (Thermo). Internal standards (EEZ-3, EEZ-4 and EEZ-6), previously contrasted with the IAEA international V-SMOW, SLAP and SLIP standards, were analysed every 3 samples. The experimental error in the determinations of $\delta^{18}O$ and $\delta^{2}H$ values is less than 0.15 and 2‰, respectively. Before the $\delta^{13}C_{(DIC)}$ analysis, water samples were filtered (0.45 μm) *in situ* by means of a syringe into 12 mL vials followed by poisoning with $HgCl_2$, in order to avoid secondary biological activity. They were then capped leaving no headspace and stored at 4 °C. In order to liberate CO_2, samples were prepared in the laboratory as follows: an aliquot of sample was injected into 12 mL vials pre-filled with He and 5 drops of 65% H_3PO_4 shaken in a Vortex agitator for 30 s. The vials were then left at room temperature between 15 and 36 h to obtain an equilibrium state (Salata et al., 2000). The CO_2 was then separated from other residual gases by chromatography using He as carrier gas in a Gas Bench system (Thermo-Finnigan, Bremen, Germany), interfaced with a mass spectrometer.

For the determination of $\delta^{34}S$ isotopic values in dissolved sulphates, SO_4^{2-} ions were previously precipitated as $BaSO_4$ and then dried, milled and homogenised in an agate

mortar. A small amount of V_2O_5 was added to an aliquot of approximately 1.5 mg of $BaSO_4$. This mixture was afterwards introduced into a Sn-capsule for its analysis in an Elemental Analyser (Carlo Elba 1500NC) through a Continuous Flow-Isotope Ratio Mass Spectrometry (EA-IRMS). During this process, the Sn-capsule was dropped by an automatic carousel into a quartz column at 1020 °C. In this moment a flash-combustion occurs due to an O_2 injection, reaching 1700 °C. The gases produced were dragged by a He stream towards a chromatographic column for the SO_2, CO_2, and NOx separation before entering to a Delta Plus XL mass spectrometer.

For the determination of $\delta^{18}O$ in dissolved sulphates, an aliquot of about 0.5 mg of $BaSO_4$ was introduced into a Ag-capsule that in turn was dropped by an automatic carousel into a ceramic column containing a glassy carbon tube at 1450 ºC to produce CO using a reverse-plumbed Pyrolisis Furnace TC/EA (Gehre et al., 2004). The CO was separated by chromatography from other minor residual gasses using a He carrier gas stream connected online with a TC/EA (Thermo-Finnigan, Bremen, Germany), before entering to a Delta Plus XL mass spectrometer.

Analytical precision is greater than ±0.3‰ for $\delta^{34}S$ values, which are expressed in relation to the V-CDT (Vienna Canon Diablo Troilite) standard. For the international IAEA-S1, NBS-127, CP-1 patterns, $\delta^{34}S_{(V\text{-}CDT)}$ values of -0.3, 20.3, and -4.5 were obtained, respectively. Analytical precision is greater than ±0.2‰ for $\delta^{18}O$ values in sulphates. Eight inhouse standards ($BaSO_4$, KNO_3, cumarine, phthalic acide, sacarose, Ag-phosphate, Benzoic acids, IAEA-C3) were used, previously prepared and calibrated against the international standards: USGS34, USGS35, IAEA-NO-3, IAEA-C3 and Benzoic acids A, B from the Indiana University.

3. 2. Carbonate samples

Samples were collected from the travertines currently forming at the emerging groundwaters from the aforementioned five wells. These samples came from: i) the El Saladillo and El Reventón travertines from the La Ermita de El Saladillo aquifer (Fig. 2A, B, C, D, E, F); ii) the El Rincón deposit from the Gañuelas aquifer (Fig. 2G, H); and iii) the Lorca and El Tiburón precipitates from the Totana aquifer (Fig. 3A, B, C, D).

The El Saladillo samples come from a continuously forming travertine precipitated by vertical accretion at the air-water interface (SAL-1 sample). Waters come out through the pipeline, falling into a pool and splashing on its walls (see Fig. 2A), where coralline-like travertines are precipitated (see Fig. 2D). Waters in the pool precipitate millimetre and laminated travertines, with stromatolitic-like structure, forming micro-terraces (see Fig. 2B, C). Afterwards, waters flow slowly by a gentle slope, accumulating them in vadose zones, where typical travertines are also precipitated around aquatic plants (SAL-2 sample). The El Reventón travertines come from a decantation conical tank (sample REV-1, see Fig. 2E), from which muds are collected for medical and beauty treatments in the spa facilities. Another sample was taken from the fillings of the thermal water pipelines (REV-2 sample, see Fig. 2F). The El Rincón sample comes from a very small carbonate deposit formed by a water leakage from the pipeline of the well installation (RINCÓN sample, see Fig. 2G, H). Finally, the Lorca and El Tiburón carbonate deposits are being formed at the exit of the pipelines recharging two different ponds, from which waters are distributed for agricultural irrigation (TIBURÓN-1 and LORCA samples, see Fig. 3A, B). Furthermore, another sample from a dry pond in the El Tiburón site (TIBURÓN-2 sample) was also taken only for petrographic characterisation (Fig. 3C, D).


A


B

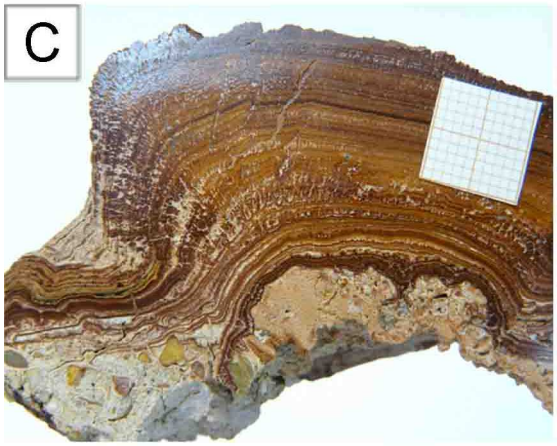
C


D


E


F


G

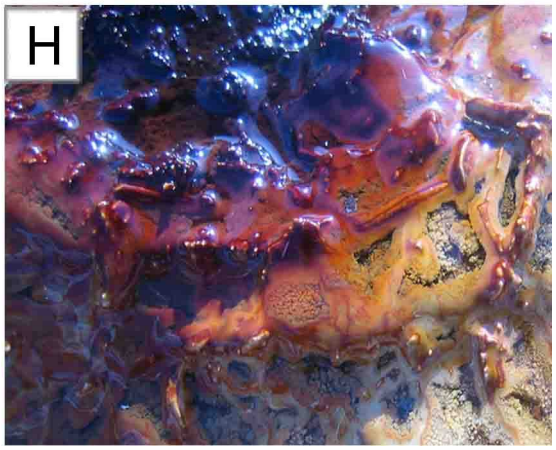
H

Fig. 2. A) Carbonate deposits formed at the emerging waters from the El Saladillo well. **B)** Detail of these carbonate deposits, showing their laminated structure and the lateral discontinuities due to simultaneous precipitation and dissolution processes (sample SAL-1). **C)** Detail of the millimetre laminated carbonates, highlighted by colour changes due to different iron proportions. Note the stromatolitic structure and the shrinkage fissures, perpendicular to the laminae, filled by probable carbonates. **D)** Carbonate with coralline-like structure formed as a result of the water splashing on the pool walls. **E)** Mud decantation conical tank at the El Reventón spa facilities, from which mud sample was taken (sample REV-1). **F)** Carbonated fillings from the thermal water pipelines in the spa installation, also showing the stromatolitic structure (sample REV-2). **G)** Surficial assemblage of the El Rincón well, where a water leakage is forming a very small reddish travertine deposit. **H)** Detail of this deposit, from which the RINCÓN sample was taken. Notice the reddish laminated structure of the travertine.

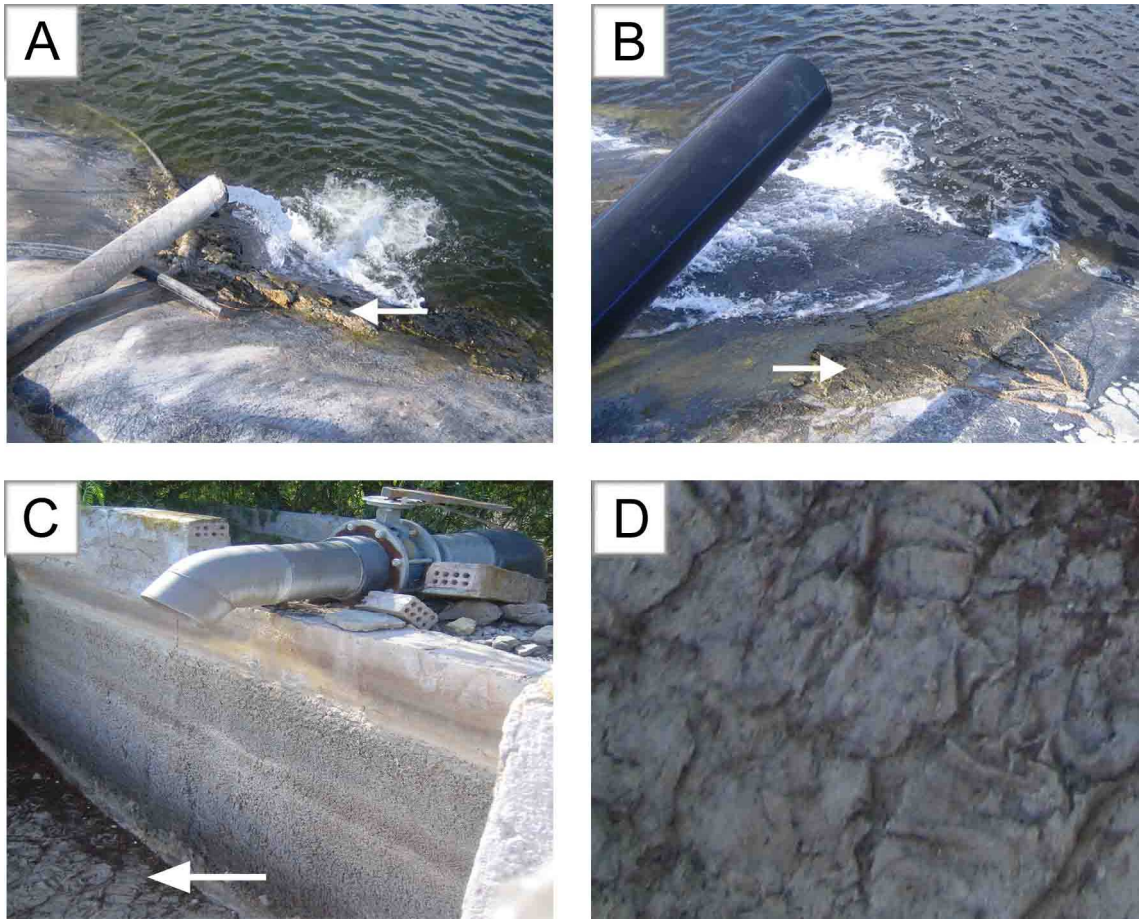

Fig. 3. A) Discharge of the El Tiburón well on an artificial plastic-covered pool, on which carbonated crust sample (TIBURÓN-1) was taken (white arrow). **B)** Similar environmental conditions under which the LORCA crust is being formed (white arrow). **C**) Dry pond at the El Tiburón site from which TIBURÓN-2 sample was collected (white arrow). **D**) Detail of C picture, where the shrinkages can be observed.

The general methodology followed for the preparation and study of the rock samples is summarised in Fig. 4.

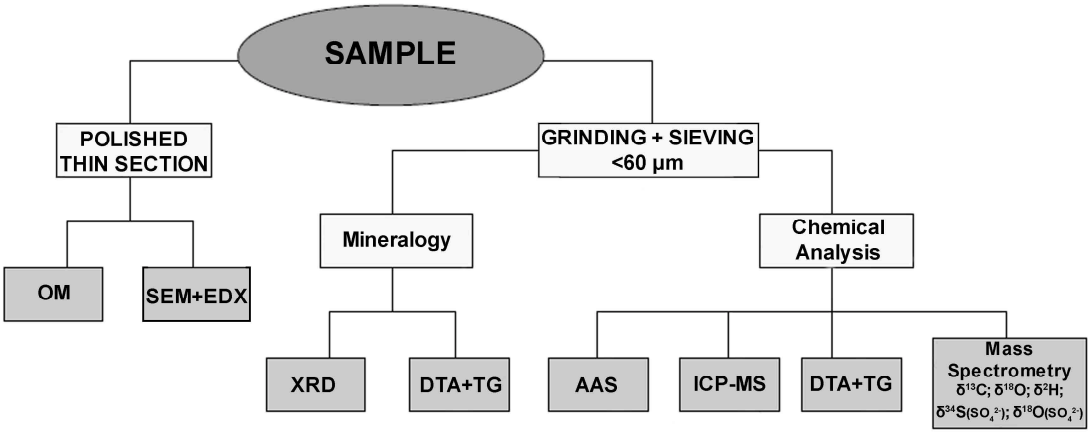

Fig. 4. Flowchart outlining the methodology followed for the preparation and study of the rock samples.

Mineralogical characterisation was firstly performed by means of X-Ray Diffraction (XRD) and Differential Thermal and Thermogravimetric Analyses (DTA+TG). The XRD analysis was done by using the non-orientated powder method on ground, sieved and homogenised <60 µm sized samples. A Philips X-Pert-MPD difractometer, CuKα radiation and a scan speed of 0.04°/s were used, the exploration range being between 2° and 70° of 2θ. The mineral phases were identified by comparing the experimental reflections spacing with those from the "Index X-Ray data for minerals (JCPD)" database.

Semi-quantitative analysis was performed using the reflecting power method of each mineral phase, initially proposed by Schultz (1964), extended by Martín Pozas (1968) and modified by Barahona (1974). The Eq. (1) and the reflections and reflecting factors listed in Table 2 were used for calculations. This method must be considered as semi-quantitative, since it has an associated error of 5% (Klug and Alexander, 1974).

$$(I/RP)_1 + (I/RP)_2 + (I/RP)_3 + ... + (I/RP)_n = 100 \quad (1)$$

Where: I = reflection intensity used for the semi-quantification of each mineral phase; RP = reflecting power selected of each mineral for the reflection used; 1,2,3..n = mineral phases identified and semi-quantified in the sample.

Table 2
Reflections and reflecting powers used for the semi-quantitative mineralogical analysis.

Mineral	Reflection (Å)	Reflecting Powers
Calcite	3.03	1
Aragonite	3.39	0.33
Dolomite	2.88	1
Quartz	3.34	1.5
Celestite	2.97	1
Gypsum	7.60	1.5
Halite	2.82	1
Phyllosilicates	4.45	0.15
K-Feldspar	3.24	1
Albite	3.18	1

Petrographic characterisation was performed by using a Zeiss West Germany Optical Microscope (OM), equipped with an Axio Cam/CC1 Zeiss camera. This technique has permitted to identify and take photomicrographs of the major and accessories minerals, as well as to recognize the main textural features. Besides this, textural characterisation and identification of the accessory minerals were complemented by Scanning Electron Microscopy (SEM). Moreover, for the illustration of these features, backscattered electron images (BEI) were taken. The equipments used were two SEM-Zeiss models: the DSM-960, coupled to an LINK (eXL) analytical system, and the EVO LS 15, coupled to an Oxford Inca Energy 350 analytical system.

Chemical analyses (Ca, Mg, Al, Fe, P and Mn) were performed by using a 735-ESE Varian Inductively Coupled Plasma Optical Emission Spectrometry (ICP-OES), while Na and K were determined by Flame Atomic Emission Spectroscopy (FAES, PE 5000, Perkin-Elmer). Trace elements, except U, Th and Zr, were determined by using a X Series II (Thermo Scientific, Bremen, Germany) Inductively Coupled Plasma Mass Spectrometer (ICP-MS). Uranium was determined by Laser Induced Kinetic Phosphorimetry (KPA-11, Chemchek Instruments Inc.), whilst Th and Zr were measured by X-Ray Fluorescence (XRF) by means of an Axios (PANanalytical) X-Ray Fluorescence Spectrometer.

An elemental analyser (Leco CS-244) was used for total C and S determinations. A standard reference soil (Soil # 1, EuroVector S.p.A., Milano, Italy) was regularly measured, in order to check the data accuracy. DTA and TG analysis were carried out using a TG/DTA 6300 system for determining H_2O^-, H_2O^+ and inorganic CO_2. Samples were heated under an air dynamic atmosphere at 10 °C/min, in the range between 30

and 950 °C. Alumina (Al_2O_3) was used as the reference inert material. The instrument was calibrated with high purity monohydrated calcium oxalate ($CaC_2O_4 \cdot H_2O$, Alfa Aesar, Karlsruhe, Germany).

For the $\delta^{13}C$ and $\delta^{18}O$ determinations of carbonates, a <60 μm sized sample aliquot was used. The aliquots were dissolved with 100% H_3PO_4 for 12 h in a thermostatic bath at 25 °C (McCrea, 1950). The CO_2 obtained was purified using a chromatographic column (continuous He flow system), and their isotopic ratios were measured in a Delta Plus XP mass spectrometer. All samples were analysed in triplicate. Carrara, EEZ-1 and EEZ-10 internal standards, previously analysed alongside NBS-18 and NBS-19 IAEA international standards, were analysed every 3 samples. The experimental error is <0.1‰ for both $\delta^{13}C$ and $\delta^{18}O$. Isotopic ratios were normalised with respect to the fractionation factors (α): 1.01044 for calcite (Kim and O'Neil, 1997), and 1.01034 for aragonite (Kim et al., 2007), both at 25 ºC. All the isotopic results were reported in the standard delta notation (δ ‰) relative to the international V-PDB standard.

4. RESULTS AND DISCUSSION

Since the current carbonates in the site are the result of the physicochemical characteristics of their parent waters, it is absolutely necessary to describe, firstly, the main features of waters from the five selected wells and, secondly, the most relevant characteristics of these carbonates.

4. 1. Water characterisation

The main physicochemical and chemical features of waters from the five sampled wells are listed in Table 3. According to their temperatures, these waters can be classified as an intermediate term between warm (20-40 ºC) and mesothermal (40-75 ºC) spring waters, following the Pentecost (2005) terminology. Furthermore, taking into account the high equivalent HCO_3^- contents, high pCO_2 (Vaselli et al., 2010; Rodrigo-Naharro et al., 2011, 2012, 2013) and $\delta^{13}C$(V-PDB) values of DIC, around -6‰ (see Table 3), these waters can be considered as parent-waters of thermogene travertines (Pentecost and Viles, 1994; Viles and Pentecost, 2007). Electrical conductivity values indicate that all waters have a very high salinity, being the Lorca, El Saladillo and El

Reventón the most saline waters. Concerning pH values, all of them are slightly acid due to the CO_2 dissolved; and Eh values indicate that the El Saladillo and El Reventón waters are more reduced in depth, while the remainders are oxidised (see Table 3). However, these values are only orientative since they were measured under atmospheric conditions.

With respect to major anions and cations, the El Saladillo and El Reventón waters have been classified as Na-Ca-SO_4^{2}-HCO_3^{-} waters, proving that these samples come from the same aquifer. The El Rincón water sample, though come from an aquifer close to that of the previous samples, shows differences concerning SO_4^{2-} and Cl^{-} contents. Consequently, it is classified as Na-Ca-HCO_3^{-}-SO_4^{2-} water. On the contrary, the El Tiburón and Lorca water samples are different between them and also very different with respect to the three previous waters, in such a way that the former is classified as Na-Mg-Cl^{-}-HCO_3^{-} water and the second as Na-Mg-Cl^{-}-SO_4^{2-} water. The charge balances of all samples are in agreement with those values considered as acceptable. Only the El Saladillo water has a charge balance >5% (see Table 3 and Fig. 5).

Trace elements have scarce significance, except Fe in the El Saladillo, El Reventón and El Rincón water samples. This fact suggests that these waters do not produce significant surficial contamination in heavy and/or toxic elements. Furthermore, among the less abundant trace elements, Sr, particularly in the El Saladillo and El Tiburón waters, can be highlighted. The presence of this element is justified by the water/rocks interaction processes, since Sr is an abundant element in the materials from the Nevado-Filábride and Alpujárride complexes (Gómez-Pugnaire et al., 1981), as well as in the filling materials of the intra-mountains Tertiary basins in the Betic Cordillera (Arana, 1973; Ortega Huertas, 1973; Ortega Huertas et al., 1973; 1974; Fernández Rubio et al., 1975; Sanz de Galdeano et al., 1976; Arana et al., 1978; Gómez-Pugnaire et al., 1981; Martin et al., 1984).

In relation to the saturation index (SI), all samples are oversaturated with respect to calcite and aragonite, particularly the El Saladillo and El Reventón waters (Fig. 6), in spite of the SI uncertainty degrees for both polymorphs ($\pm$0.35), according to Plummer and Busemberg (1982); Deutsch et al. (1982); Back et al. (1983); Nordstrom and Ball (1989) and Tena et al. (1990).

Table 3
Physicochemical and chemical features of waters from which the carbonates studied are precipitating.

Physicochemical Features[a]	El Saladillo (4)[b]	El Reventón (4)	El Rincón (4)	El Tiburón (4)	Lorca (4)
T (ºC)	45.60	45.73	35.93	29.93	23.35
EC (µS/cm) "in situ"	9387.50	8905.00	5385.00	7530.00	10970.00
pH "in situ"	6.75	6.50	6.38	6.25	6.77
Eh (mV)	-45.8	-267.8	50.7	129.6	120.3
HCO_3^- (mg/L)	2009.34	1992.53	2159.45	1946.73	732.40
SO_4^{2-} (mg/L)	3529.47	3458.01	1774.75	1262.91	2929.98
Cl^- (mg/L)	1128.50	1049.50	203.00	1380.75	2487.50
F^- (mg/L)	2.89	2.58	1.41	0.62	0.64
PO_4^{2-} (mg/L)	25.26	24.12	23.50	32.53	14.95
Br^- (mg/L)	2.00	2.20	0.52	2.05	4.35
NH_4^+ (mg/L)	4.80	7.50	0.77	0.30	0.23
Ca^{2+} (mg/L)	553.65	452.39	354.78	400.47	824.27
Mg^{2+} (mg/L)	251.45	204.70	121.45	419.06	528.53
Mg^{2+} / Ca^{2+}	0.45	0.45	0.34	1.04	0.64
Na^+ (mg/L)	2353.56	2249.79	1176.74	985.72	1552.79
K^+ (mg/L)	83.81	75.90	35.32	42.66	19.66
Fe^{3+}_{total} (mg/L)	3831.05	2376.18	1125.00	407.64	340.00
SiO_2 (mg/L)	16.60	16.35	13.02	20.15	21.32
Sr (µg/L)	8.10	3.13	2.76	6.22	3.27
Mn (µg/L)	0.053	0.029	0.022	0.653	0.252
Li (µg/L)	2.89	2.93	1.01	1.89	0.47
Ba (µg/L)	0.01	0.02	0.01	0.02	0.03
Be (µg/L)	0.002	0.002	0.0005	0.0001	0.0003
U (µg/L)	0.03	0.003	0.011	0.013	0.012
Th (µg/L)	0.0001	0.0001	0.0001	0.0001	0.003
Tl (µg/L)	0.0002	0.00001	0.0003	0.00004	0.00005
Al (µg/L)	0.08	0.04	0.23	0.16	0.80
As (µg/L)	0.04	0.02	0.02	0.01	0.02
Co (µg/L)	0.001	0.0004	0.0005	0.008	0.003
Mo (µg/L)	0.001	0.001	0.001	0.002	0.002
Ni (µg/L)	0.014	0.008	0.012	0.015	0.024
Sb (µg/L)	0.0002	0.0001	0.0003	0.00001	0.00005
V (µg/L)	0.014	0.013	0.003	0.018	0.036
Zr (µg/L)	0.02	0.01	0.03	0.02	0.03
Zn (µg/L)	0.02	0.01	0.03	0.02	0.03
Cu (µg/L)	0.01	0.01	0.01	0.01	0.01
Cr (µg/L)	0.04	0.04	0.01	0.06	0.11
Pb (µg/L)	0.0003	0.0001	0.0004	0.0003	0.01
Se (µg/L)	0.01	0.01	0.01	0.02	0.26
$\delta^{13}C_{(V\text{-}PDB)}$ (‰)	-5.58	-6.38	-6.41	-5.62	-6.36
$\delta^{18}O_{(V\text{-}SMOW)}$ (‰)	-6.90	-6.27	-6.94	-7.02	-6.63
$\delta^{2}H_{(V\text{-}SMOW)}$ (‰)	-39.50	-34.70	-38.85	-42.58	-38.24
$\delta^{34}S$ (SO_4^{2-})(‰)	17.73	19.16	19.01	16.60	10.89
$\delta^{18}O$ (SO_4^{2-}) (‰)	14.77	15.68	16.23	14.02	10.70
Balance (%)	8.52	2.14	1.25	0.75	3.88
Hydrochemical Classification	Na-Ca-SO_4^{2-}	Na-Ca-SO_4^{2-}	Na-Ca-SO_4^{2-}-HCO_3^-	Na-Mg-Cl^--HCO_3^-	Na-Mg-Cl^--SO_4^{2-}
Saturation Index (SI)	Calcite (0.96) and Aragonite (0.83)	Calcite (0.62) and Aragonite (0.49)	Calcite (0.44) and Aragonite (0.30)	Calcite (0.23) and Aragonite (0.09)	Calcite (0.48) and Aragonite (0.33)

[a] These values are the averages of four measurements done during different field campaigns.
[b] The number of water samples were 4.

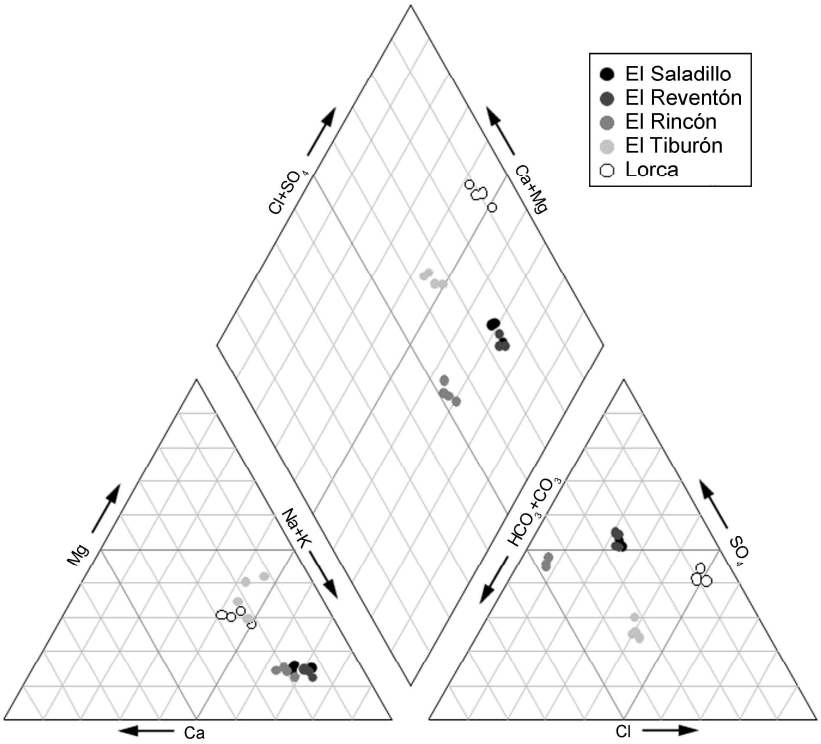

Fig. 5. Piper-Hill diagrams where the 5 types of water are plotted.

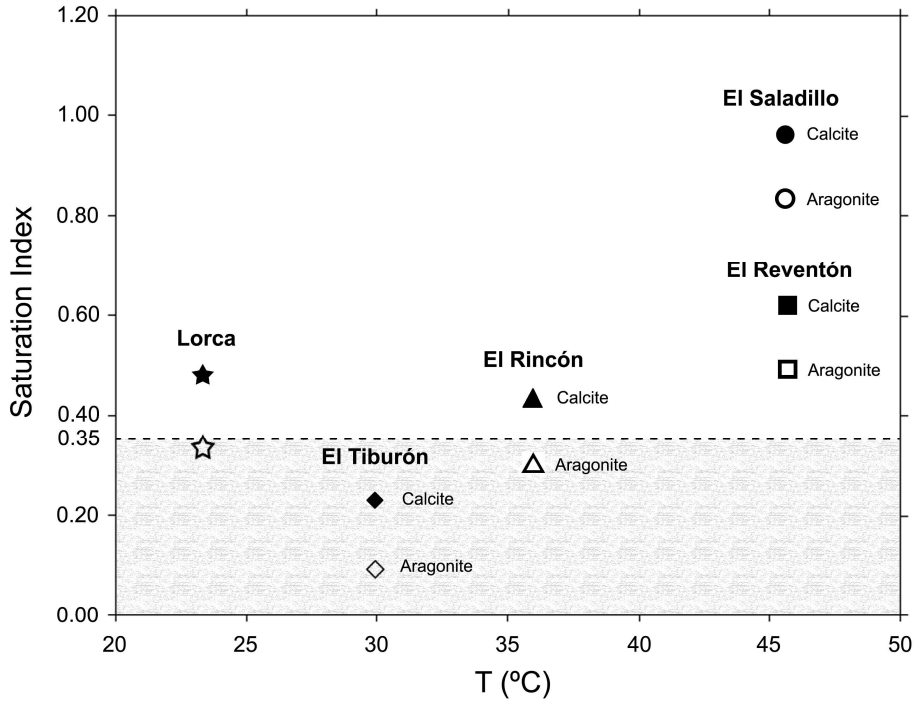

Fig. 6. Saturation Index of the water samples with respect to calcite and aragonite. Shaded area corresponds to the positive uncertainty range for both calcite and aragonite.

The isotopic signature of C from DIC ($\delta^{13}C_{(V\text{-}PDB)}$) of these water samples varies from -5.6 to -6.4‰, which is compatible with CO_2 from the terrestrial mantle. However, these values can be also reached considering a mixture of C from the oxidation of the vegetation cover and dissolution or thermal decomposition of limestone (Fig. 17).

On the other hand, the $\delta^{18}O_{(V\text{-}SMOW)}$ and $\delta^{2}H_{(V\text{-}SMOW)}$ values of these water samples were represented in relation to the Craig (1961) Meteoric Water Line (MWL) (Fig. 7). According to this plot, all samples are located above the MWL, similarly to that found in meteoric waters from the Almería-Murcia region (Delgado, 1994; Cerón et al., 1998; Delgado and Reyes, 2004). These waters are characterised by an excess in D that can be due to rainfalls from clouds originated in the Mediterranean Sea or in continental regions (Gat and Carmi, 1970). This is corroborated considering that these water samples are plotted between the MWL ($\delta^{2}H = 8\times\delta^{18}O + 10$) and the hypothetical Mediterranean Meteoric Water Line M-MWL ($\delta^{2}H = 8\times\delta^{18}O + 22$) (see Fig. 7).

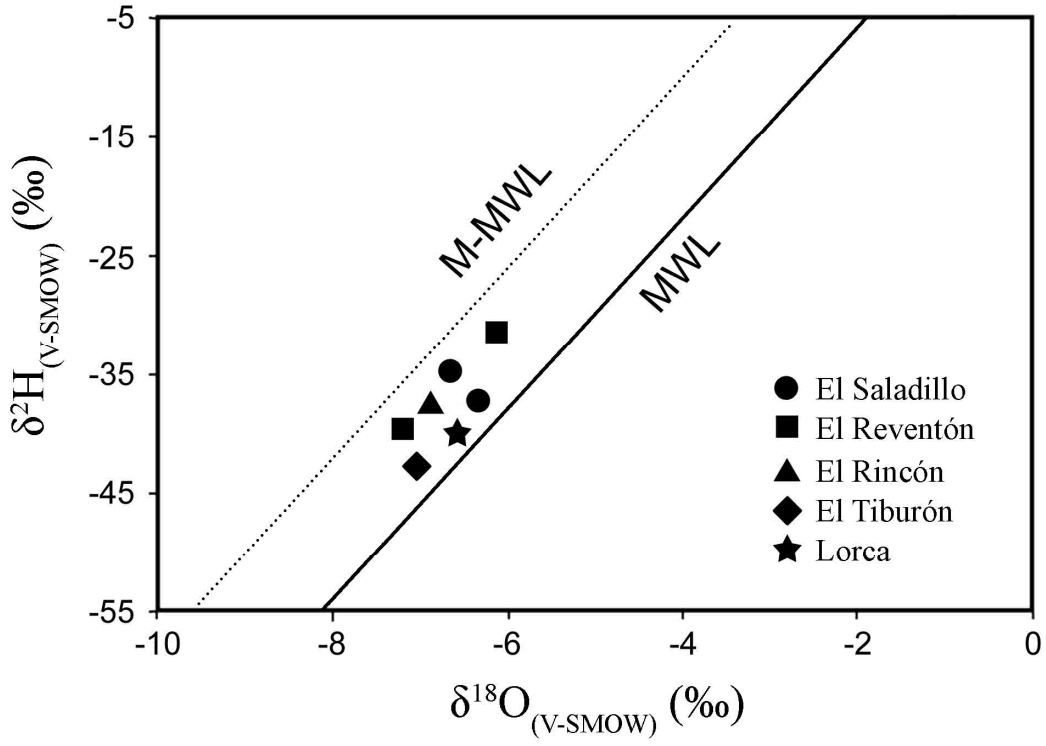

Fig. 7. Representation of the $\delta^{18}O_{(V\text{-}SMOW)}$ and $\delta^{2}H_{(V\text{-}SMOW)}$ values of water samples in relation to the Craig (1961) Meteoric Water Line (MWL) and the hypothetical Mediterranean Meteoric Water Line (M-MWL).

Another explanation could be given whether an ^{18}O impoverishment in the water is considered. This phenomenon is related to the CO_2-H_2O isotopic interchange, since CO_2 is enriched in ^{18}O. Though this possibility is unusual due to the high difference between water and gas densities, these small isotopic changes could be explained when there is abundant CO_2 as happen in the five wells sampled. This isotopic interchange can occurs particularly during periods in which water was relatively retained in the well pipelines, where minor degassing occurs. Furthermore, it is not discardable the existence, in the site, of significant amount of supercritical CO_2 in depth, favouring the ^{18}O impoverishment of the groundwaters.

The $\delta^{34}S_{(V\text{-}CDT)}$ values of the total dissolved sulphates range between 10.9 and 19.2‰, the most higher values being in agreement with those corresponding to the Messinian marine gypsum existing in the SE Spain (Longinelli, 1979). Concerning the $\delta^{18}O_{(V\text{-}SMOW)}$, ranging between 10.7 and 16.2‰, the higher values being in equilibrium with the isotopic oxygen and temperatures of the sampled waters (Fig. 8), indicating high residence times. Only the lowest $\delta^{18}O_{(V\text{-}SMOW)}$ value (10.7‰ in Lorca) indicates higher temperature in depth. In this last case, the dissolution of the Messinian marine gypsum must be discarded, since the isotopic values ($\delta^{18}O$ and $\delta^{34}S$) are different with respect to the remaining samples. However, this value is in agreement with those obtained from the hydrothermal sulphates existing in this area or with those measured in the giant gypsum crystals from the El Pulpí cave, located at about 70 km towards SW from this site (García-Guinea et al., 2002). The $\delta^{34}S_{(V\text{-}CDT)}$ value is relatively low (10.9‰), indicating a possible oxidation of sulphur.

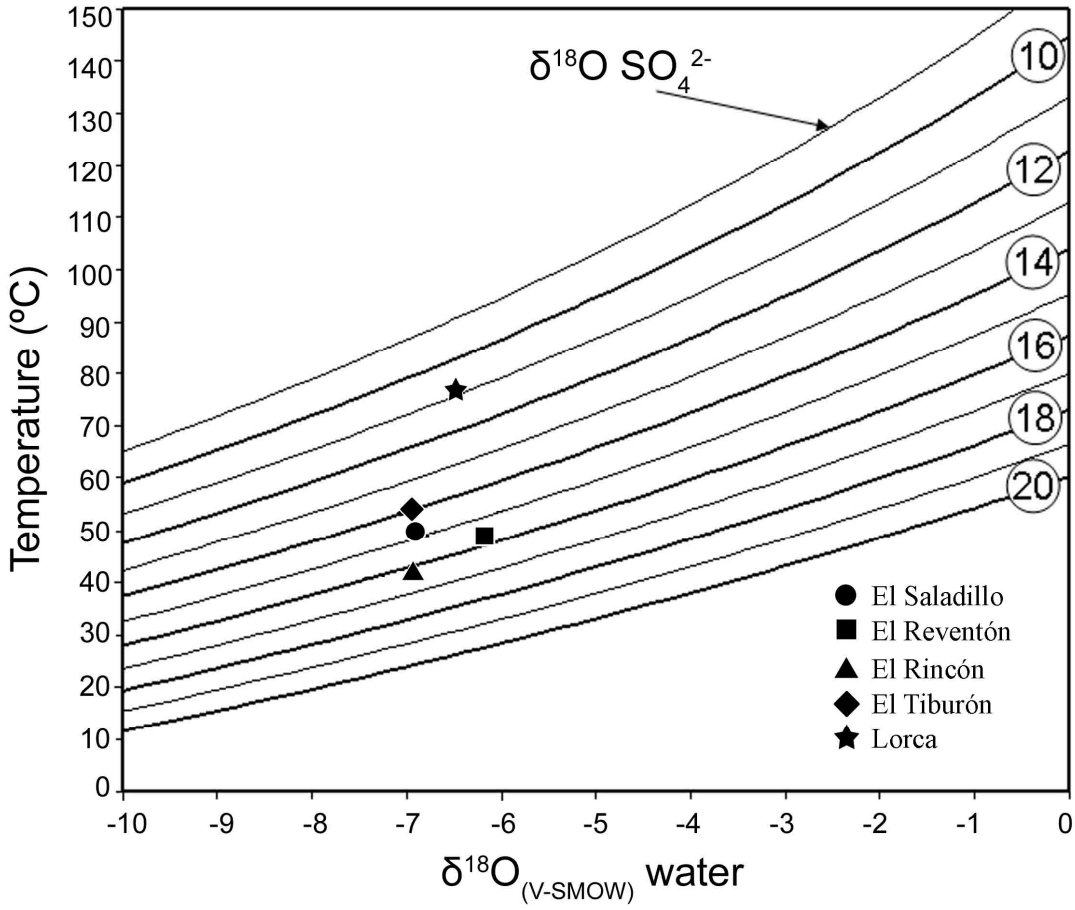

Fig. 8. Curves represent theoretical temperatures for sulphate-oxygen system (9 to 20‰) in isotopic equilibrium with meteoric and marine waters (-10 to 0‰). Equation of Kusakabe and Robinson (1977) has been used for calculations of the represented curves. The black symbols represent the $\delta^{18}O_{(V\text{-}SMOW)}$ values of sulphates and their respective current parent-waters for the El Saladillo, El Reventón, El Rincón, El Tiburón and Lorca wells. From these variables it was deduced the equilibrium temperatures, which are: 49.8, 48.4, 41.9, 53.3 and 76.8 ºC, respectively. The two first values are practically in agreement with those measured in their corresponding sampling points: S and R (see Table 1), indicating a rapid water rise and the absence of mixtures with shallow aquifers. However, the remaining calculated temperatures are much higher than those measured in their respective wells: El Reventón, El Tiburón and Lorca (see Table 1), indicating non-isotopic equilibrium. Nevertheless, calculated temperatures for El Rincón (41.9 ºC) and El Tiburón (53.3 ºC) are similar to those of other hot springs in the region, indicating, consequently, cooling processes or contamination with shallow cold waters. Calculated temperature (76.8 ºC) for Lorca well is extremely higher than its measured temperature, indicating an inherited isotopic value of higher temperatures or even the dissolution of marine sulphates (9.4‰ $_{V\text{-}SMOW}$). However, marine/sedimentary sulphates in this area (Messinian gypsum) have $\delta^{34}S_{(V\text{-}CDT)}$ values between 20 and 24‰ (Longinelli, 1979), whilst the obtained value (10.8‰) is far from the abovementioned values for the Messinian gypsum, ruling out this last hypothesis.

4. 2. Carbonate characterisation

Before describing the main features of the rock forming carbonates, it is convenient to advertise that, in general, description will be done considering samples individually, except when mineralogical composition (major minerals) is treated.

4. 2. 1. Mineralogy

The semi-quantitative mineralogical composition (Table 4) indicates that the: i) SAL-1, SAL-2 and REV-1 samples are mainly composed of aragonite, with minor goethite and dolomite, though in REV-2 both calcite and aragonite are present in similar proportions; ii) RINCÓN and LORCA samples are essentially formed by calcite, with minor quartz; and iii) TIBURÓN-1 is a mixture of aragonite and calcite, with minor quartz, whilst the TIBURÓN-2 is aragonitic in nature, with minor calcite, dolomite and quartz.

Table 4.
Semi-quantitative mineralogical composition of the samples, obtained by XRD.

Sample	Aragonite	Calcite	Dolomite	Goethite	Quartz	Total
SAL-1	89	3	---	8	---	100
SAL-2	90	3	3	4	---	100
REV-1[a]	92	8	---	---	---	100
REV-2	44	56	---	---	---	100
RINCÓN	---	96	---	---	4	100
TIBURÓN-1	61	34	---	---	5	100
TIBURÓN-2	82	11	3	---	4	100
LORCA	---	100	---	---	---	100

[a] REV-1: Mud from the decantation conical tank. Traces of halite (NaCl) and thenardite (Na_2SO_4) were detected in this sample, probably formed during the sample drying.

Minor minerals were only determined in SAL-1, SAL-2 and REV-2 samples due to their compactness, by using SEM+EDX on polished thin sections, previously coated with C and/or Au. Among these minerals, botryoidal Fe-oxy-hydroxides like goethite is highlighted (Fig. 9A). Furthermore, probably inherited, idiomorphic and partially altered pyrite (Fig. 9B) and early diagenetic framboidal pyrite, either oxidised or not, were also detected, indicating probable bacterial activity and changes in the Eh condition during the carbonate precipitation, respectively (Fig. 9C, D). Iron carbonate and probable ankerite, Fe-Ca-(Mn), were also identified (Fig. 9E, F). Celestite (Fig. 9G, H), barite and sphalerite are also present into the carbonate mass.

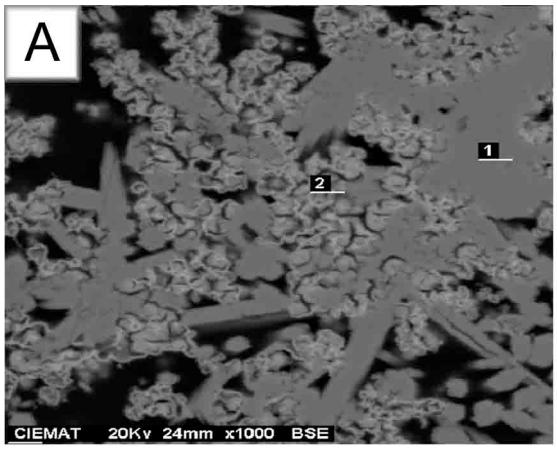
A
1
2
CIEMAT 20Kv 24mm x1000 BSE

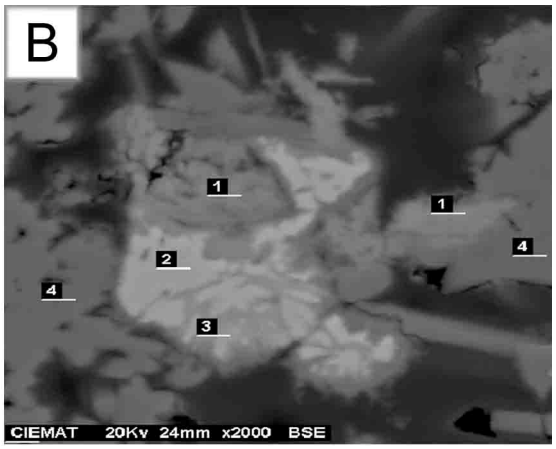
B
1
1
2
4
4
3
CIEMAT 20Kv 24mm x2000 BSE

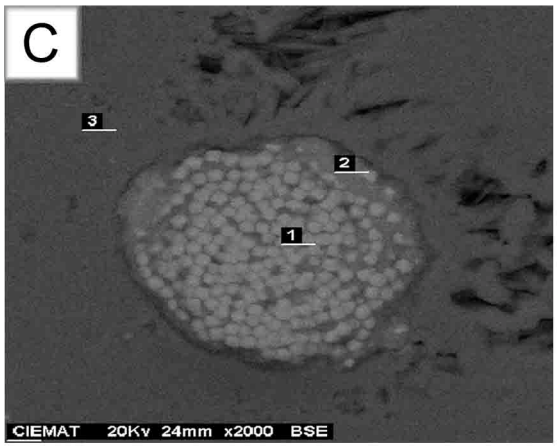
C
3
2
1
CIEMAT 20Kv 24mm x2000 BSE

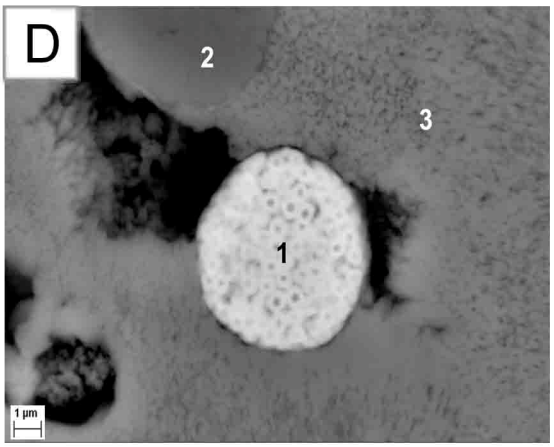
D
2
3
1
1 µm

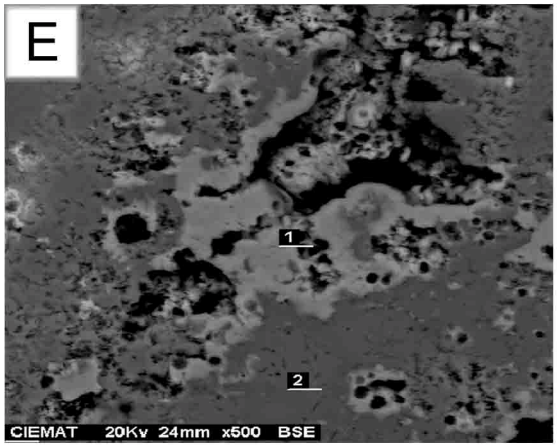
E
1
2
CIEMAT 20Kv 24mm x500 BSE

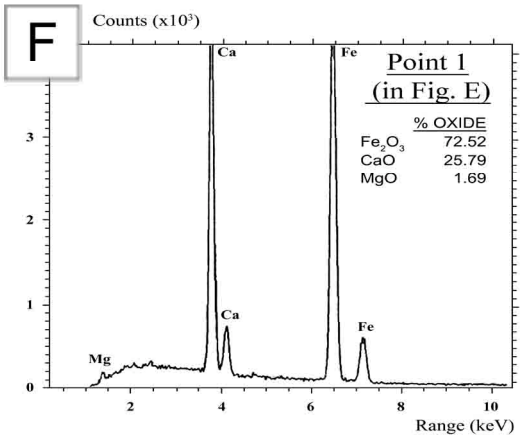
F
Counts (x10³)
Ca
Fe
Point 1
(in Fig. E)
% OXIDE
Fe2O3 72.52
CaO 25.79
MgO 1.69
Ca
Fe
Mg
0
1
2
3
2
4
6
8
10
Range (keV)

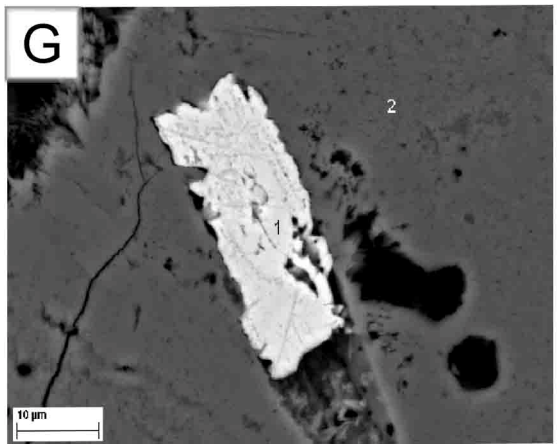
G
2
1
10 µm

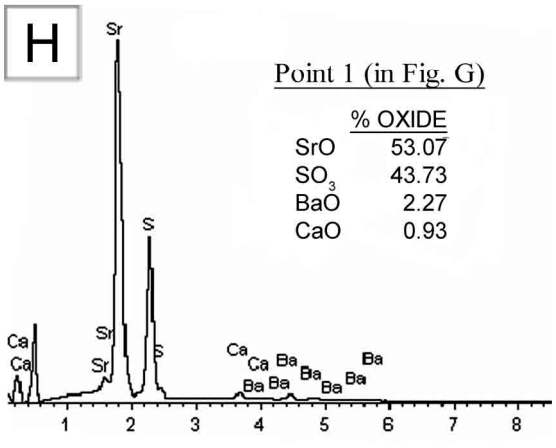
H
Sr
Point 1 (in Fig. G)
% OXIDE
SrO 53.07
SO3 43.73
BaO 2.27
CaO 0.93
S
Ca
Ca
Sr
Sr
S
Ca
Ca
Ba
Ba
Ba
Ba
Ba
Ba
1
2
3
4
5
6
7
8

Fig. 9. A) BEI of botryoidal Fe-oxy-hydroxides (2), probably goethite. **B**) BEI of a sub-idiomorphic, inherited and partially altered pyrite crystal (3). **C**) BEI of framboidal pyrite (1), surrounded by $CaCO_3$, probably aragonite (3). **D**) BEI of framboidal pyrite totally oxidised (1); quartz (2); $CaCO_3$ (3). **E**) BEI of Fe and Fe-Ca-(Mn) carbonates, the latter being probably ankerite (1). **F**) EDX spectrum of the ankerite (Point 1). **G)** BEI of a xenomorphic crystal of celestite (1), embedded into a carbonate mass, probably aragonite (2). **H)** EDX spectrum of the celestite crystal.

It is worth mentioning the presence, as minor minerals, of tiny polymetallic nodules composed of Mn, Co, Ni, Cu and Zn, with minor S, Mg, Ca and Al. These nodules are coated by Fe-oxy-hydroxides and surrounded by $CaCO_3$, probably aragonite. Their morphological features and their relationships with the carbonate mass suggest that they are inherited and transported by the well-waters. Furthermore, their chemical composition is similar to that of the polymetallic nodules currently forming in the oceanbasin floor, near the oceanic ridges (Fig. 10A, B).

As inherited minerals, dolomite (Fig. 10C, D), calcite, apatite, quartz, plagioclase, monazite (Fig. 10E, F), epidote (Fig. 10G, H), zircon (Fig. 11A), ilmenite (Fig. 11B, C), probably plates of graphite, rutile and micas (Fig. 11D, E) were detected.

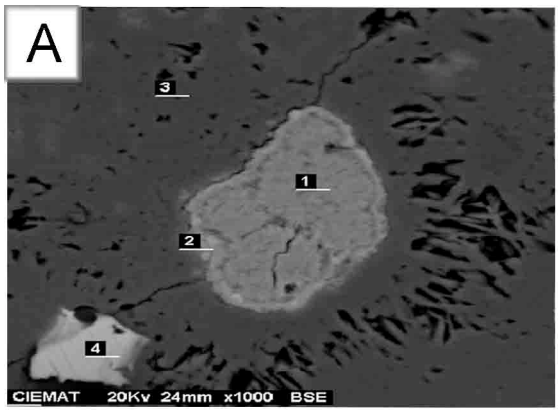
A
3
1
2
4
CIEMAT 20Kv 24mm x1000 BSE

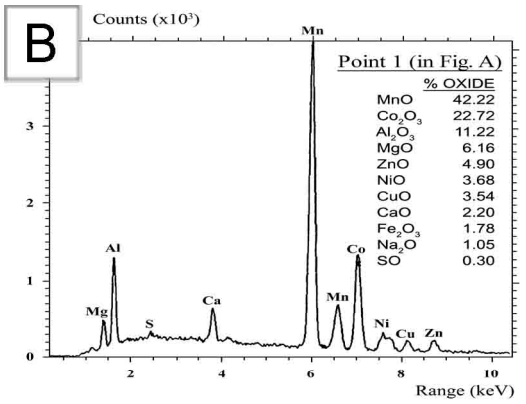
B
Counts (x10³)
Point 1 (in Fig. A)
% OXIDE
MnO 42.22
Co2O3 22.72
Al2O3 11.22
MgO 6.16
ZnO 4.90
NiO 3.68
CuO 3.54
CaO 2.20
Fe2O3 1.78
Na2O 1.05
SO 0.30
Mg
Al
S
Ca
Mn
Co
Ni
Cu
Zn
Range (keV)

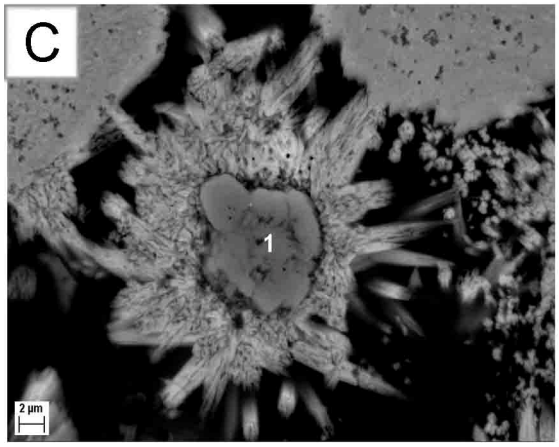
C
1
2 µm

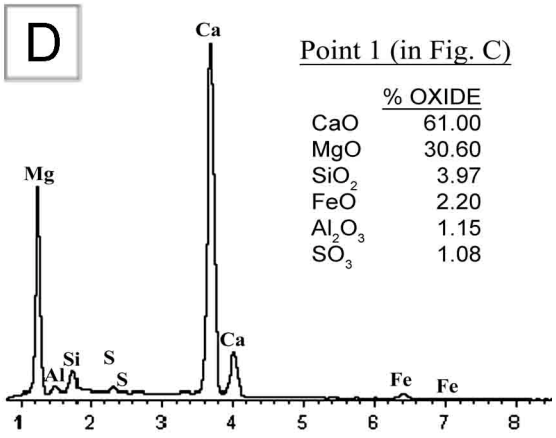
D
Point 1 (in Fig. C)
% OXIDE
CaO 61.00
MgO 30.60
SiO2 3.97
FeO 2.20
Al2O3 1.15
SO3 1.08
Mg
Si
Al
S
S
Ca
Ca
Fe
Fe

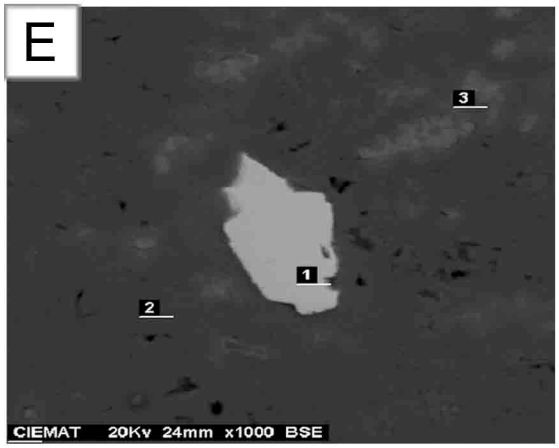
E
3
1
2
CIEMAT 20Kv 24mm x1000 BSE

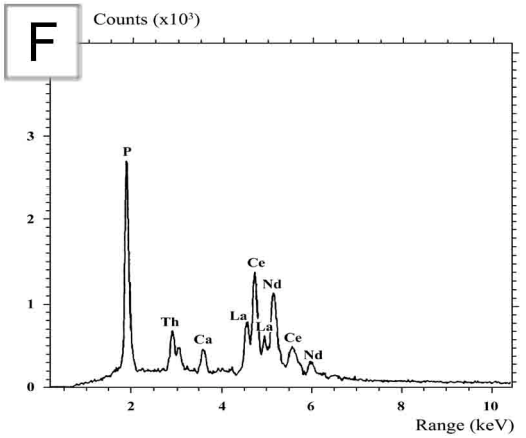
F
Counts (x10³)
P
Th
Ca
La
Ce
Nd
La
Ce
Nd
Range (keV)

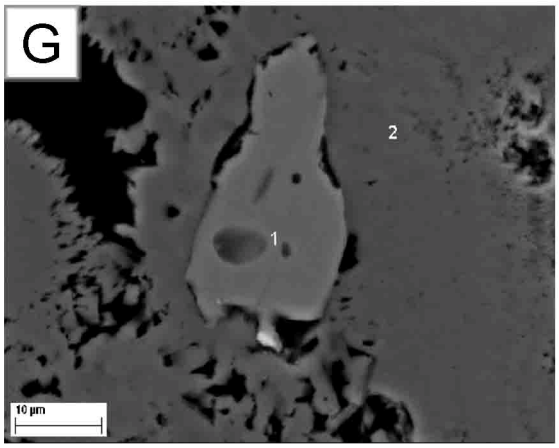
G
2
1
10 µm

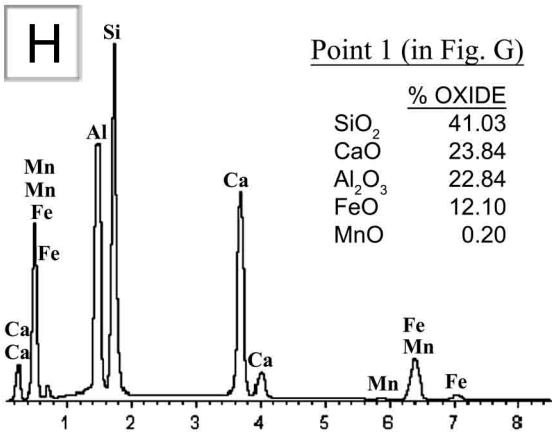
H
Point 1 (in Fig. G)
% OXIDE
SiO2 41.03
CaO 23.84
Al2O3 22.84
FeO 12.10
MnO 0.20
Si
Al
Mn
Mn
Fe
Fe
Ca
Ca
Ca
Ca
Fe
Mn
Mn
Fe

Fig. 10. A) BEI of an inherited polymetallic nodule (1), constituted of Mn, Co, Ni, Cu and Zn, embedded into the carbonate mass, probably aragonite (3); Fe-oxyhydroxides (2) and a particle of Fe metallic (4), probably from the well pipeline. **B)** EDX spectrum of the polymetallic nodule. **C)** BEI of an inherited aggregate of dolomite crystals (1) surrounded by acicular carbonates, probably aragonite (2). **D)** EDX spectrum of the inherited dolomite. **E)** BEI of an inherited xenomorphic monazite crystal (1) embedded into the carbonate mass, probably aragonite (2). **F)** EDX spectrum of the Th-rich monazite from image E. **G)** BEI of an inherited xenomorphic epidote crystal (1), embedded into the carbonate mass, probably aragonite (2). **H)** EDX spectrum of the epidote crystal.

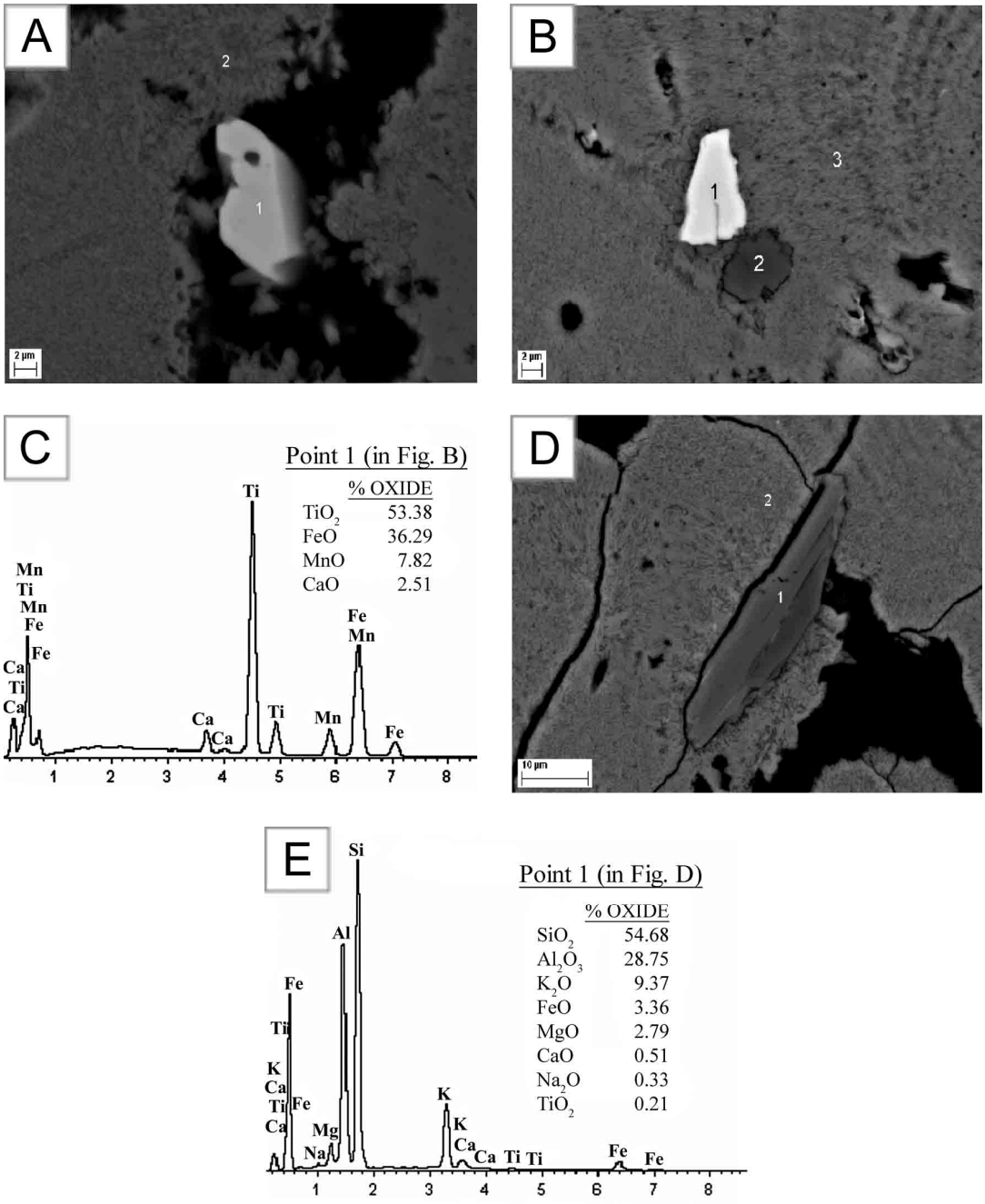

Fig. 11. A) BEI of an inherited sub-idiomorphic zircon crystal (1) embedded into the carbonate mass, probably aragonite (2). **B**) BEI of an inherited xenomorphic ilmenite crystal (1), embedded into the carbonate mass, probably aragonite (3); inherited dolomite (2). **C**) EDX spectrum of Mn-rich ilmenite. **D**) BEI of inherited mica (1) surrounded by the carbonate mass, probably aragonite (2). **E)** EDX spectrum of the inherited mica, probably muscovite.

4. 2. 2. Petrography

Samples SAL-1 and SAL-2 correspond to a travertine body that is active at present. Microscopic observations reveal that this travertine is composed of an alternation of porous and dense horizons. The first are formed by dendritic branches appearing as a shrub-like structure (Fig. 12A), composed of upward-radiating branches (Fig. 12B), which really are individual bacteria forming clumps (Chafetz and Folk, 1984). The dense horizons are composed of fine-grained micrite partially recrystallised to sparite. The porosity appears encrusted by acicular aragonite needles sized between approximately 10-100 μm of diameter (Fig. 12C, D). Similar textural characteristics were observed in REV-2 sample that is formed by calcite and aragonite (Fig. 12E, F).

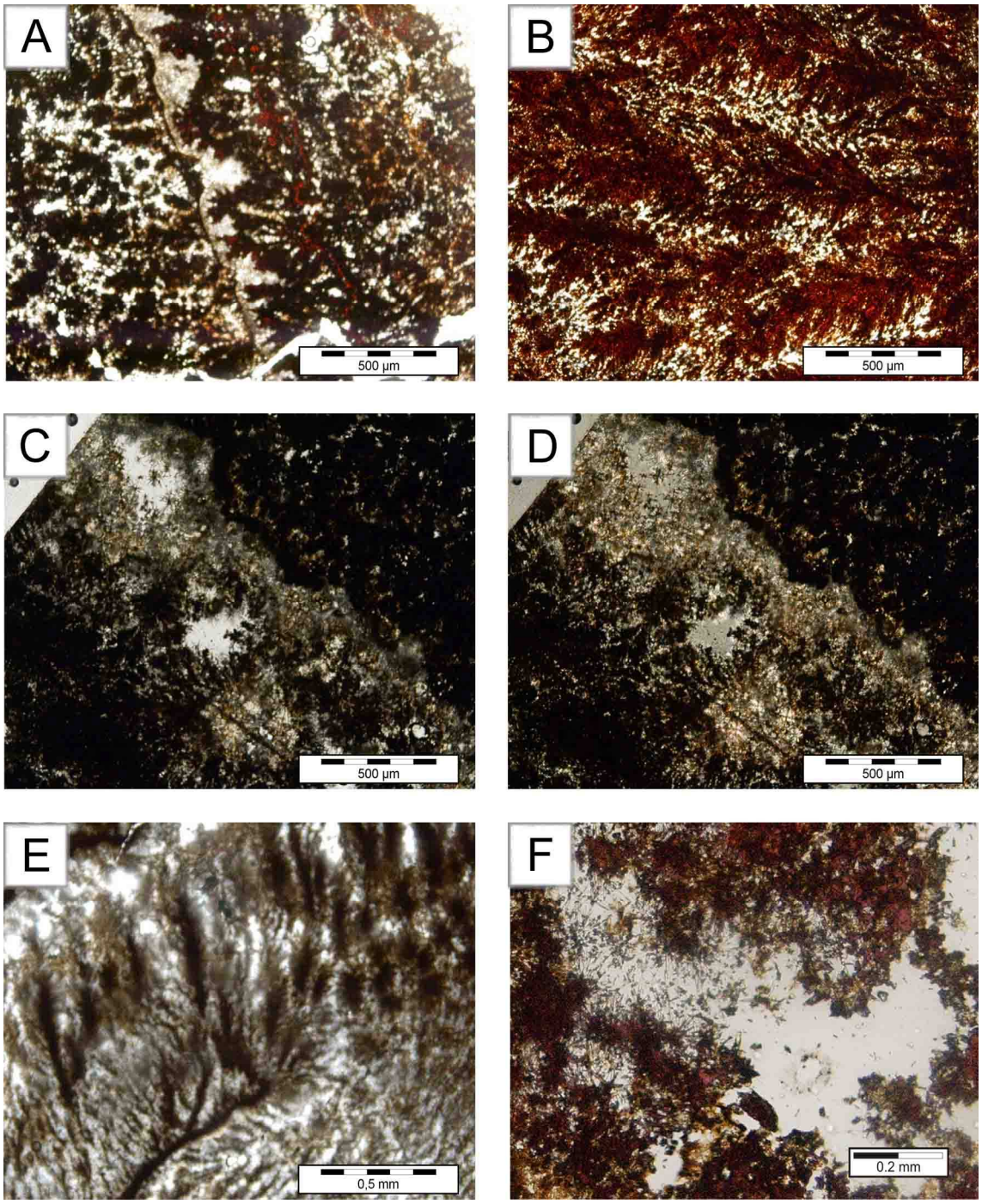

Fig. 12. SAL-1 and SAL-2 samples: A) Repetitive thin dendritic micrite layers intercalated with sparite. **B)** Upward radiating branches composed of chains of individual bacteria clumps (top to the left of the photomicrograph). **C)** Detail of the porous horizon, where aragonite needles appear filling porosity. **D)** Idem in crossed nicols. **REV-2 sample: E)** Dendritic calcite (bacterial clumps) layers showing abundant framework porosity. **F)** Detail of the framework porosity partially filled by aragonite needles.

For a comprehensive study of the textural features of these samples, thin and polished sections were observed by SEM+EDX. Under low magnification, the carbonate layers are essentially formed by $CaCO_3$, with more or less Fe, ranging

between 5.7 and 41% of Fe_2O_3 (Fig. 13A, B, C, D), which is responsible for the reddish colour of the layer and, in general, of the sample (see Fig. 2C). The Fe content variations are reflected in the grey tonalities in the SEM image (see Fig. 13A). Under higher magnification, carbonates show acicular and/or fibrous-radiating textures, which are typical of the aragonite. In the first case, pores formed by the aragonite needles framework are filled by botryoidal Fe-oxy-hydroxides (see Fig. 10A), whilst in the second texture, aragonite shows isolated star morphologies (Fig. 14). Furthermore, all layers contain significant amounts of S and Sr (see Fig. 13B, C, D). Sulphur, as SO_4^{2-}, and Sr probably replace CO_3^{2-} and Ca, respectively, in the aragonite structure.

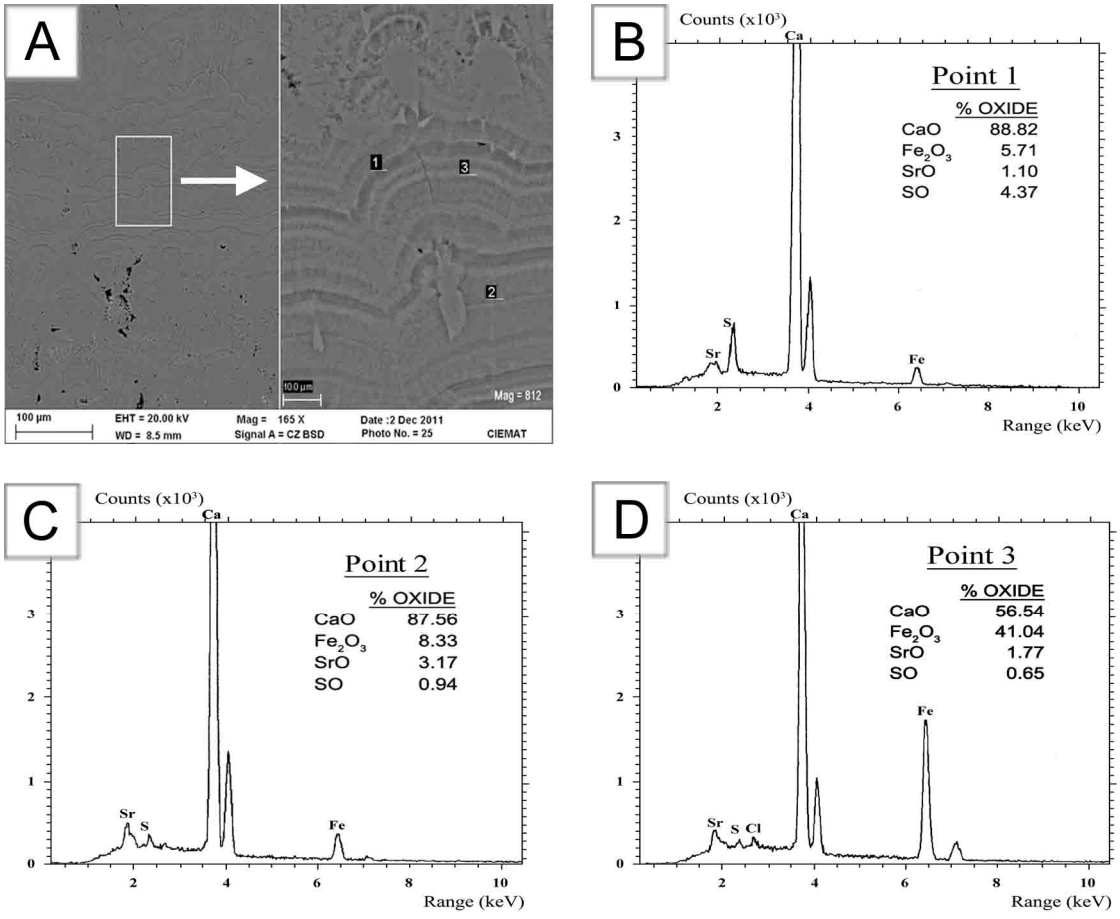

Fig. 13. A) BEI of the laminated stromatolitic carbonates (SAL-1 sample). Fe-rich layers are in lighter greys. 1, 2 and 3 are the analysed points by EDX. **B, C, D)** EDX spectra of points 1, 2, 3, in which Fe, Sr and S are detected in significant proportions.

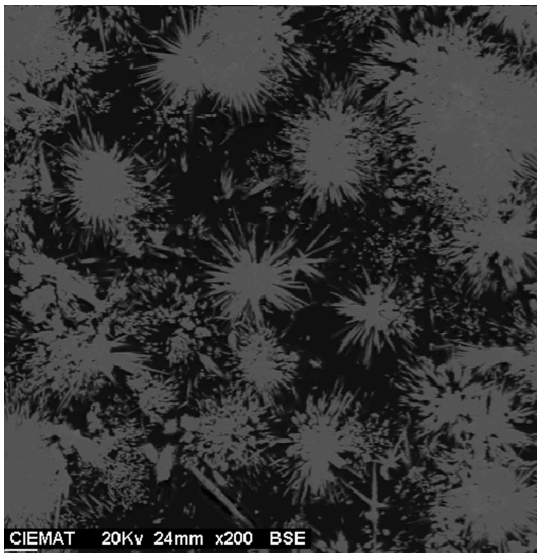

Fig. 14. BEI of radiating fibrous aggregates of aragonite needles (SAL-1 sample).

Aragonite precipitation is preferentially produced at temperatures higher than 40 ºC and from $CaCO_3$ oversaturated parent-waters (Chafetz and Folk, 1984). Furthermore, aragonite precipitation is triggered by: i) sudden CO_2 degassing of parent-waters, originating the oversaturation in $CaCO_3$ (Jones and Renault, 2010); ii) the presence of high Sr or Mg contents in the parent-waters (Kitano, 1962; Jones and Renault, 2010); iii) a Mg/Ca ratio >1 (Folk, 1974), though the importance of this parameter is controversial (Jones and Renault, 2010); iv) the presence of organic matter (Kitano and Hood, 1965; Meyer, 1984); and v) relatively high levels of Fe^{2+} and SO_4^{2-} ions. According to this, it can be stated that the El Saladillo and El Reventón parent-waters satisfy all the abovementioned triggering factors, except for the Mg/Ca ratio, which is approximately 0.5. Consequently, it can be suggested that these parent-waters have the most suitable physicochemical features for the aragonite precipitation in this natural system. Concerning Fe, the El Saladillo and El Reventón parent-waters are reduced and, therefore, Fe in solution will be present as Fe^{2+}, though it was measured as Fe^{3+} because the analytical procedure used. In addition, quick oxidation occurs at the well-water discharge points, as reflected in the close relationship between aragonite and goethite precipitation.

Petrographycally, SAL-1, SAL-2 and REV-2 samples have similar textural features, with alternating milimetric shrubs and micritic sheets forming stromatolitic-like structures adapted to the substratum surface. The shrubs sheets are formed by columnar aggregates growing perpendicular to the substratum. These textures/structures were

already described by Folk et al. (1985) and Freytet and Verecchia (1998) in travertine terraces and runoff sites. Nevertheless, these authors described sheets of several centimetres thickness separated by discontinuities. These stromatolitic-like structures are formed in microbial mat environments (Farmer and Des Marais, 1994). The discontinuities observed in the stromatolitic travertines are attributed to temporal variations in their growth pattern. That is, they are related to the lower rate and even cessation of the $CaCO_3$ precipitation during humid periods, mainly in spring and autumn seasons.

The RINCÓN sample shows similar textural features to those of SAL-1, SAL-2 and REV-2 samples. It appears, as well, characterised by a structure in microterracetes (see Fig. 2H), with abundant plants in the substratum. Calcite is the predominantly carbonate phase, forming stromatolitic-like structures as previously described for samples SAL-1, SAL-2 and REV-2 (Fig. 15A). The existence of plants is reflected by the imprints of hollow tubes from stems and roots formed by the decay of the organic matter (Fig. 15B). Consequently, this sample could be the result of direct calcite precipitation from its corresponding parent-water, though its textural features are similar to those of SAL-1, SAL-2 and REV-2, which paradoxically are generally aragonitic in nature.

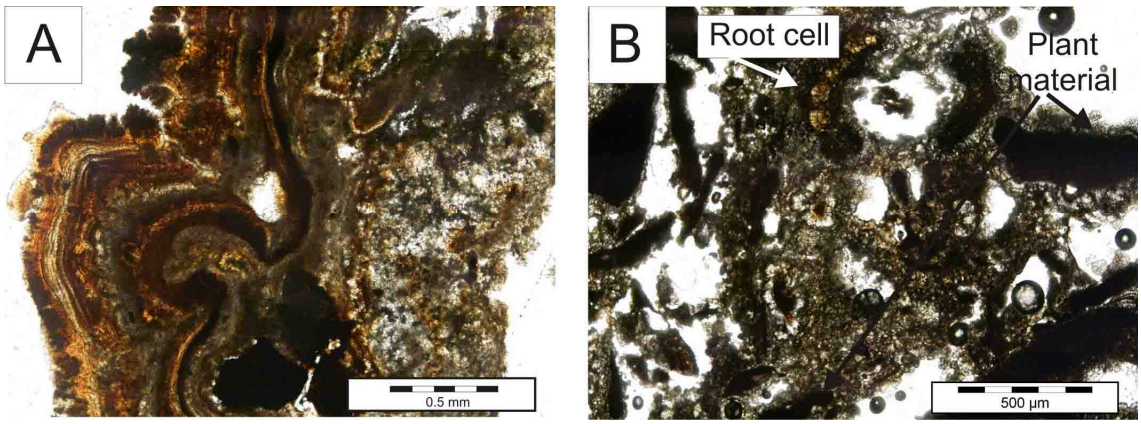

Fig. 15. A) Micrite nucleus formed by bacterial clumps surrounded by micrite and sparite laminae, which have irregular and sinuous shapes. **B)** Micritic bacterial clumps partially dissolved, with abundant plants and stem and root cells.

Both TIBURÓN-1 and LORCA samples are being formed under similar conditions as previously explained. They are forming at the water discharge points of the El Tiburón and Lorca wells over artificial plastic-covered pools. However, though both carbonate samples are formed from slightly different parent-waters, petrographically are

very similar and, therefore, they are described together. These samples are composed of micritic layered crusts with filaments growing perpendicularly to them and to the plastic substratum. These filaments are mineralised with sparite and then encrusted by carbonate micrite (Fig. 16A, B, C, D). The pores in the rock are distributed among the filaments. Bacterial platelets of various centimetres in length and around 100 μm in thickness appear coated by aragonite crystal aggregates, only at the bottom of the platelets (see Fig. 16C). Diatoms and calcified bubbles are also present (see Fig. 16B), as well as some micritic clumps.

Mineralogically both samples are quite different since the first is formed by calcite and the second is a calcite and aragonite mixture, the parent–waters being also quite different (see Table 3). In these cases, Cl^- and Sr seem to be the main factors controlling the polymorph precipitation, in such a way that the Lorca parent-water is the most suitable for calcite precipitation, compared to the El Tiburón one. Petrographically both samples are composed of a bio-film mat of green algae with solitary filaments formed in a semi-stagnant water body. Calcified bubbles, platelets and bacterial growth forming sheets reflect an alternation of rapid and slow growing rate periods.

The TIBURÓN-2 sample, which was collected from the walls and floor of a current dry pond, was formed under stagnant water conditions followed by desiccation processes. It is essentially composed of aragonite with minor calcite, dolomite and quartz. This sample can be described as a micritic crust (Fig. 16E, F) composed of irregularly distributed and oriented filaments moulds (see Fig. 16E, F), either isolated or densely encrusted, forming a lamellar structure. These filaments are more easily observed in the lightest zones of the thin sections. Furthermore, calcified bubbles and diatoms were also recognised (Fig. 16G, H). This sample is formed from parent-waters with very different physicochemical features in relation to those of the El Saladillo and El Reventón parent-waters. Thus, the El Tiburón parent-water is cold, oxidised, slightly acid, and with a Mg/Ca ratio of approximately 1 (see Table 3).

Finally, all parent-waters of the studied carbonates are highly enriched in Cl^-, which is paradoxically considered as an inhibitor of aragonite precipitation (Jones and Renault, 2010).

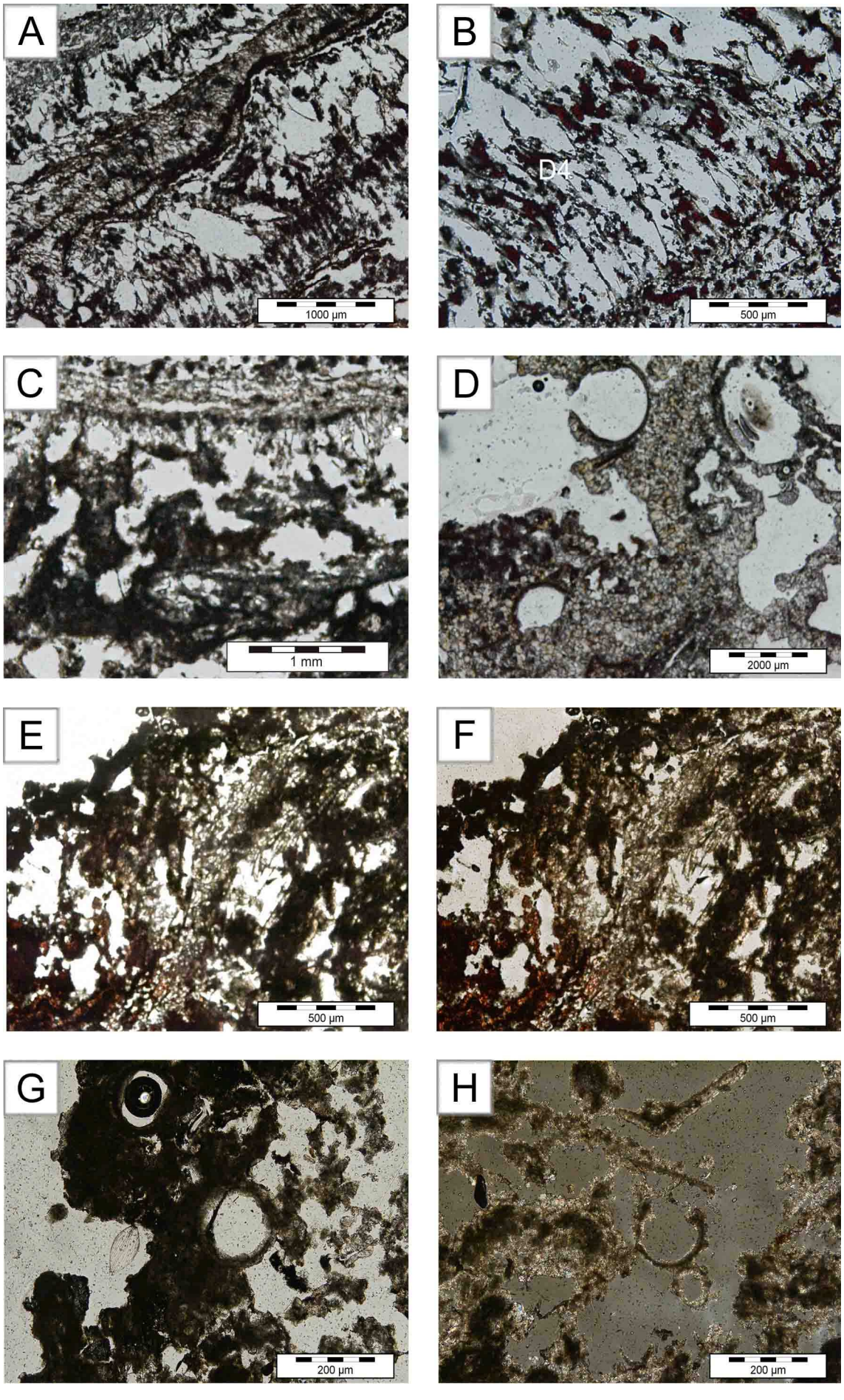
A
1000 µm
B
D4
500 µm
C
1 mm
D
2000 µm
E
500 µm
F
500 µm
G
200 µm
H
200 µm

Fig. 16. LORCA and TIBURÓN-1 samples: A) Photomicrograph showing the laminated micritic texture of the carbonate crust. The bacterial clumps form wavy to horizontal sheets forming cycles. Bacterial filaments grow perpendicularly to the horizontal sheets. **B)** Photomicrograph showing the spaces among the bacterial filaments. Notice that these spaces are empty of any organic or inorganic material. **C)** Platelets coated by calcite crystals. **D)** Bacterial film around a gas bubble. **TIBURÓN-2 sample: E)** Photomicrograph showing micritic carbonate crust composed of bacterial filaments. **F)** Idem in crossed nicols, where the bacterial filaments are better observed in the light zones of the sample. Notice the alternation of the dark and light zones. **G)** Photomicrograph where micrite clumps with diatoms and calcified bubbles are observed**. H)** Photomicrograph of a thin section where aragonitic clumps are probably being transformed into calcite (crossed nicols).

4. 2. 3. Elemental and isotopic geochemical characterisation

Chemical composition of some representative carbonate samples, including major, minor and trace elements, is listed in Table 5. Data corresponding to samples SAL-1 and REV-1 are similar to those from thermogene travertines (Pentecost, 2005; Prado-Pérez, 2011). Setting aside the high content in CaO and inorganic CO_2, the most relevant oxides are: i) Fe_2O_3 in samples SAL-1 and REV-1, which would justify their high As concentration, since both elements have a high geochemical affinity; ii) SO_3 in all samples is justified by the existence of minor sulphate minerals, as well as by the presence of SO_4^{2-} substituting CO_3^{2-} in aragonite (see Fig. 13B, C, D); iii) organic CO_2 is particularly high in sample TIBURÓN-1, probably due to the high biological current activity; iv) detected Ba in some samples would be related to the minor barite observed in them; and v) Sr is also justified by the presence of celestite in the samples, as well as replacing Ca in the aragonite structure (see Fig. 13B, C, D). In addition, Zn and U must also be highlighted, both probably associated with Fe-oxy-hydroxides. These geochemical anomalies suggest minor, but detectable, mobilization processes of more or less toxic elements by the El Saladillo and El Reventón well-waters, both characterised by relatively high temperatures (~46 ºC) and low acidity (pH 6.2). Cerium, La and Zr are associated with detrital minerals dragged by well-waters, such as monazite and zircon (see section 4.2.1).

Table 5
Major and minor and trace elements in some representative carbonate samples.

Element	SAL-1	REV-1	TIBURÓN-1	RINCÓN	LORCA
SiO_2 (%)	1.35	0.00	6.91	0.01	0.01
Al_2O_3 (%)	0.19	0.53	1.97	2.52	0.39
$Fe_2O_{3(total)}$ (%)	**13.24**	**15.55**	1.94	3.18	0.19
MgO (%)	0.15	0.38	1.57	2.03	1.20
MnO (%)	0.00	0.01	0.24	1.58	0.93
CaO (%)	47.17	38.05	36.47	43.58	56.15
Na_2O (%)	0.45	2.05	1.05	0.57	0.25
K_2O (%)	0.06	0.11	0.50	0.78	0.11
TiO_2 (%)	0.01	0.01	0.09	0.09	0.02
P_2O_5 (%)	0.04	0.07	0.07	0.09	0.18
H_2O^- (%)	1.58	2.50	2.50	2.00	2.67
$CO_{2(inorg.)}$ (%)	32.04	33.08	32.48	40.03	32.24
$CO_{2(org.)}$ (%)	1.93	3.99	11.08	0.89	3.22
SO_3 (%)	0.60	2.17	1.56	1.08	1.43
SrO (%)	0.89	1.28	0.82	1.05	0.35
TOTAL	99.70	99.79	99.26	99.48	99.36
As (ppm)	**349**	**305**	<3	13	<0.1
Ba (ppm)	21	38	**80**	**200**	36
Be (ppm)	20	13	<3	1.1	<0.1
Ce (ppm)	**4.8**	<3	<3	**15**	1.8
Co (ppm)	<3	<3	<3	3.8	1.5
Cr (ppm)	<3	8.0	14	20	5.4
Cu (ppm)	<3	<3	7.0	-	3.8
La (ppm)	**15**	**34**	**33**	**11**	1.7
Mo (ppm)	<3	<3	<3	1.8	0.34
Ni (ppm)	≤3	<3	<3	27	15
Sn (ppm)	<3	N.D.[a]	N.D.	≤0.1	<0.1
V (ppm)	<3	<3	<3	14	<6.0
W (ppm)	≤3	N.D.	N.D.	1.1	≤0.1
Y (ppm)	<3	<3	<3	4.0	1.2
Zn (ppm)	**50**	**15**	**25**	**74**	**20**
Zr (ppm)	8.7	10	N.D.	3	1.2
U (ppm)	**1.6**	**2.2**	**7.8**	**4.6**	**1.6**
Li (ppm)	30	44	45	24	12

[a] N.D.: Non Determined.

On the other hand, in order to corroborate whether the carbonates from the investigated sites precipitate in isotopic equilibrium, as well as to elucidate the more probable origin of C, the isotopic signatures ($\delta^{18}O$ and $\delta^{13}C$) of these minerals were determined. For SAL-1 laminated carbonate sample, 12 analyses were done on aliquots taken according to Fig. 17. In addition, 3 analyses of samples collected in the same site

during different field campaigns were also performed. For samples REV-1 and LORCA, 3 and 2 analyses were done, respectively; whilst for RINCÓN and TIBURÓN-1, only 1 analysis for each sample was realised (Table 6).

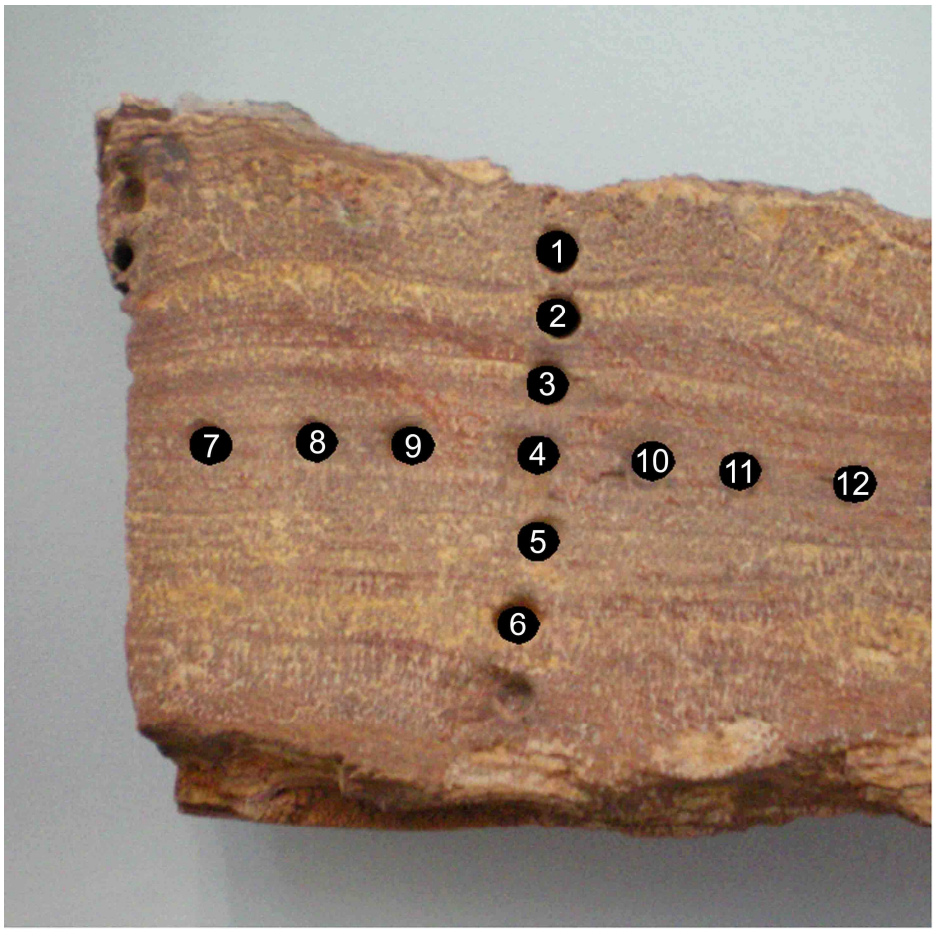

Fig. 17. Location of the aliquots taken from SAL-1 laminated carbonate sample. Aliquots were taken by using a dentist's drill.

Table 6
Isotopic signatures ($\delta^{13}C_{(V\text{-}PDB)}$ and $\delta^{18}O_{(V\text{-}PDB)}$) of carbonate samples, expressed as ‰.

Sample	Isotopic values	Nº of analyses	Min. V.[a] (‰)	Max. V.[b] (‰)	Average (‰)	Standard deviation (‰)
SAL-1	$\delta^{18}O_{(V\text{-}PDB)}$	15	-12.59	-10.46	-11.15	0.53
	$\delta^{13}C_{(V\text{-}PDB)}$	15	-3.09	-1.19	-1.78	0.49
REV-1	$\delta^{18}O_{(V\text{-}PDB)}$	3	-9.07	-8.47	-8.78	0.3
	$\delta^{13}C_{(V\text{-}PDB)}$	3	-1.19	-0.33	-0.74	0.43
LORCA	$\delta^{18}O_{(V\text{-}PDB)}$	2	-5.52	-5.39	-5.46	0.09
	$\delta^{13}C_{(V\text{-}PDB)}$	2	2.73	3.19	2.96	0.33
RINCÓN	$\delta^{18}O_{(V\text{-}PDB)}$	1	---	---	-7.89	---
	$\delta^{13}C_{(V\text{-}PDB)}$	1	---	---	-1.04	---
TIBURÓN-1	$\delta^{18}O_{(V\text{-}PDB)}$	1	---	---	-4.71	---
	$\delta^{13}C_{(V\text{-}PDB)}$	1	---	---	3.07	---

[a] Min. V.: Minimum value.
[b] Max.V.: Maximum value.

The $\delta^{18}O_{(V\text{-}PDB)}$ average value of SAL-1 is -11.15‰, while those for REV-1 and RINCÓN are -8.78 and -7.89‰, respectively. Less negative average values were measured in LORCA and TIBURÓN-1 samples, being -5.39 and -4.71‰, respectively. Regarding the $\delta^{13}C_{(V\text{-}PDB)}$ values, SAL-1, REV-1 and RINCÓN samples show very similar average values between -0.74 and -1.78‰, whereas LORCA and TIBURÓN-1 samples are enriched in ^{13}C, both very close to 3.1‰.

The $\delta^{18}O$ isotopic signatures of carbonates and their parent-waters were used for the calculation of temperatures under which these carbonates are precipitating. Calculations were done by using the equilibrium equations relating the isotopic composition to temperature for both aragonite/calcite-water systems. Before calculations, a comprehensive revision of the specialised literature was done (Grossman and Ku, 1986; Patterson et al., 1993; Thorrold et al., 1997; White et al., 1999; Böhm et al., 2000; Zhou and Zheng, 2003; Kim et al., 2007; Epstein et al., 1953; Craig, 1965; Friedman and O'Neil, 1977; Anderson and Arthur, 1983; Kim and O'Neil, 1997; Owen et al., 2002), in

order to apply the most suitable equations for both systems. As a result, the Kim et al. (2007) and Kim and O´Neil (1997) equations (Eq. 2 and Eq. 3) were used for the aragonite/calcite-water systems, respectively. This election was made on the basis that the carbonates studied have a continental and inorganic origin, with some biological inputs.

$$1000ln\alpha_{\text{aragonite-water}} = 17.88 \pm 0.13\ (10^3T^{-1}) - 31.14 \pm 0.46 \qquad (2)$$

$$1000ln\alpha_{\text{calcite-water}} = 18.03\ (10^3T^{-1}) - 32.42 \qquad (3)$$

Where: α is the fractionation factor of aragonite and calcite, respectively; and T is the temperature expressed as ºK.

Applying Eq. 2 to aragonite samples (SAL-1, REV-1 and TIBURÓN-1) and Eq. 3 to calcite samples (RINCÓN and LORCA), the estimated temperature range for the carbonates precipitation (Fig. 18A, B, C, D, E) is listed in Table 7, in which both, the estimated precipitation and the current temperatures of their respective parent-waters, have also listed for comparison. These data show that, in general, the estimated precipitation temperatures are lower than the parent-water temperatures, except for the El Saladillo site, in which both are very similar. These differences are consistent since the parent-water temperatures are going down before carbonate precipitation. This difference is extremely broad in the El Tiburón and Lorca sites, where precipitation temperatures are even lower than the environmental temperature. These values are normal and predictable, since the precipitation of carbonates is associated with irrigation pools, which are exposed to water evaporation (see Fig. 3), and the consequent enrichment of ^{18}O.

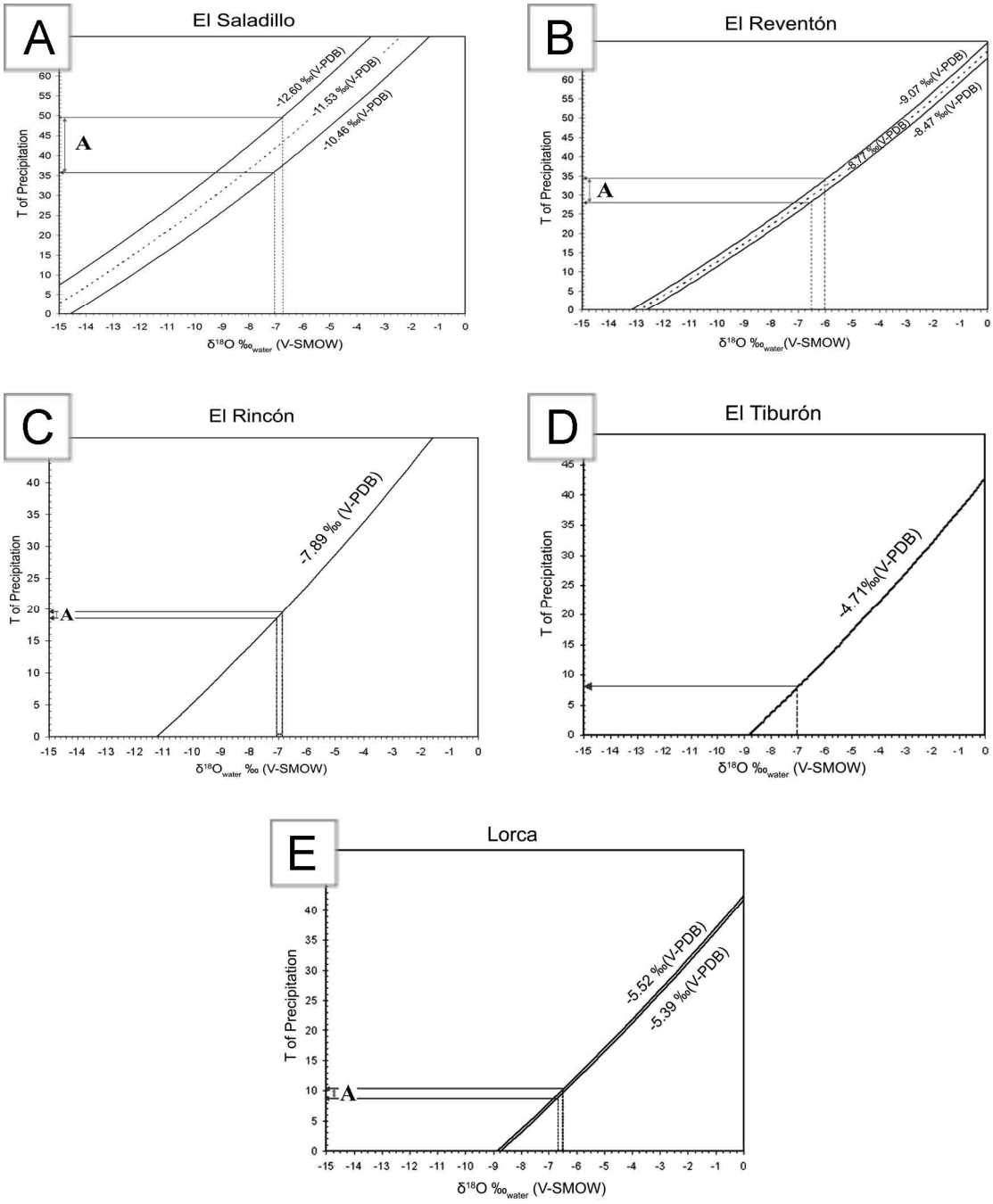

Fig. 18. Graphical representation of the $\delta^{18}O_{(V\text{-}PDB)}$ values of carbonates (aragonite and calcite) in equilibrium with their parent-waters with different isotopic signature (Kim et al., 2007; Kim and O´Neil, 1997), and the $\delta^{18}O_{(V\text{-}SMOW)}$ values of the current parent-waters for the El Saladillo (A); El Reventón (B); El Rincón (C); El Tiburón (D); and Lorca (E) sites. From these variables, the temperature ranges under which the current carbonates are precipitating was deduced. The ranges are represented by the vertical "A" segment.

Table 7
$\delta^{18}O_{(V\text{-}PDB)}$ values of carbonates and their parent-waters, calculated temperatures (range and average values) for carbonates, and measured temperatures for parent-waters.

Sample	$\delta^{18}O_{(V\text{-}PDB)}$ Aragonite/Calcite [Range Values (‰)]	$\delta^{18}O_{(V\text{-}SMOW)}$ Parent-Water [Range Values (‰)]	Calculated Temperature [Range Values (‰)]	Calculated Average T (ºC)	Measured Parent-Water T (ºC)	Dif.[a]
SAL-1	[-12.60/-10.46]	[-7.05/-6.75]	[36.0/49.5]	42.8	44.7	1.9
REV-1	[-9.07/-8.47]	[-6.50/-6.04]	[28.0/34.3]	31.2	45.9	14.7
TIBURÓN-1	-4.71	[-7.03/-7.02]	8.0	8.0	30.1	22.1
RINCÓN	-7.89	[-7.04/-6.85]	[18.7/19.5]	19.1	36.3	17.2
LORCA	[-5.39/-5.52]	[-6.71/-6.54]	[8.7/10.2]	9.5	23.3	13.8

[a] Dif.: Difference between the calculated and measured temperatures.

Given that the relationship existing between temperature and the isotopic fractionation of C in the carbonate-water system is very low, $\delta^{13}C$ isotopic signatures were not used for estimating precipitation temperature of these carbonates. However, this isotopic signature generally indicates the source of C and can also reflect any change in the environmental conditions under which the precipitation of carbonates occurs. In fact, the original $\delta^{13}C$ signature of DIC in waters can be modified by any physical and/or biological processes occurring in the system before the carbonate precipitation (Berner, 1997; Shackleton and Opdyke, 1973). As a consequence, the $\delta^{13}C$ values of the analysed carbonates are mainly controlled by the isotopic signature ($\delta^{13}C$) of DIC of their parent-waters, when precipitation occurs in equilibrium.

Analysed samples have $\delta^{13}C_{(V\text{-}PDB)}$ values between -3.09 and 3.19‰ with an average value of 0.95‰ (see Table 7). These values have been represented in Fig. 19, in which other $\delta^{13}C$ values from the main possible sources of C in the region are also represented for comparison. From this Figure, C of the analysed carbonates has an important inorganic component. However, the isotopic signature of C from DIC of their parent-waters could be explained either as a mixture of both C from organic material degradation (respiration) and C from the dissolution or decarbonatation of the Alpujárride and Nevado-Filábride carbonate rocks; or related to deep CO_2 leakages, probably from the terrestrial mantle. This last possibility would imply that deep CO_2 would be the major component of the abovementioned mixture. Nevertheless, the

$^{3}He/^{4}He$ isotopic ratio (see section 2) of free gases supports the hypothesis that C from DIC has a cortical origin, as a result of a mixture of decomposition of carbonates, with some influence of organic and mantelic C. According to Romanek et al. (1992) and Turi (1986), the isotopic composition of carbonates is enriched in 1 or 2 δ units with respect to $\delta^{13}C$ of DIC. As a consequence, carbonates from the El Saladillo site show the more coherent data, since their $\delta^{13}C$ values are approximately 3‰ more positive than their corresponding DIC. However, the enrichment in ^{13}C in the remaining samples is significantly higher, which could be related to CO_2 degassing processes (Valero-Garcés et al., 1999), or to biological activity (Fouke et al., 2000). During photosynthesis, algae preferentially fixed ^{12}C, causing enrichment in ^{13}C of DIC and in their corresponding carbonates. This reasoning allows suggesting that $\delta^{13}C$ values of both DIC from parent-waters and their corresponding carbonates could be used as good tracers for CO_2 leakages from an artificial deep geological storage of this greenhouse gas. Isotopic signature ($\delta^{13}C$) of CO_2 from organic fuel combustion is very negative, around -30‰, which can be relatively preserved in the CO_2 leaked, either as free gas or DIC, despite the possible water/rock/gas interaction processes that could occur during its escape towards the atmosphere.

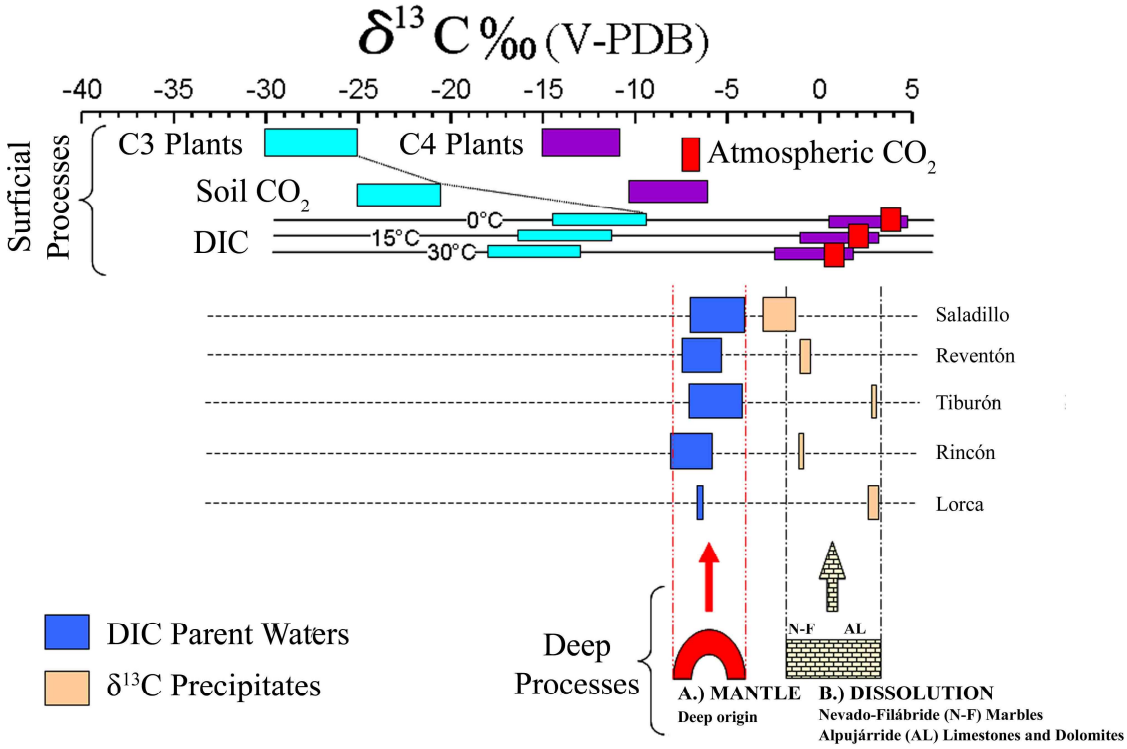

Fig. 19. Graphical representation of the isotopic signature $\delta^{13}C$ of the carbonates analysed. The more frequent isotopic values for C3 and C4 plants are represented at the top (Deines, 1980). CO_2 in soils is enriched in approximately 4.5‰ with respect to biomass (Cerling, 1984; 1991). The isotopic difference between CO_2 values in soils and DIC depends on temperature and pH, being close to 0‰ at pH~5, though is relatively independent at pH~7 (Romanek et al., 1992). As the carbonates precipitate from neutral waters, it can be discarded the pH effect, considering, therefore, only the temperature effect. Thus, theoretical calculations of the $\delta^{13}C$ of DIC and calcite/aragonite can be done considering: i) the calcite/aragonite-bicarbonate system is relatively simple and independent of temperature, and taking into account that both carbonates are always enriched in 1 or 2 δ units with respect to their respective DIC (Romanek et al., 1992; Turi, 1986); and ii) the equation relates the isotopic fractionation of C for calcite/aragonite-CO_2 system and temperature (Romanek et al., 1992). For this graphical representation temperatures of 0, 15 and 30 °C have been considered (Modified from Reyes et al., 1998; Delgado and Reyes, 2004). Inorganic C sources from deep processes are represented at the bottom of the figure.

5. SUMMARY AND CONCLUSIONS

Once data from the different components of the studied natural system have been exposed and discussed, the most relevant features used to achieve the proposed objectives can be summarised as follows:

Regarding groundwaters, 4 hydrofacies were recognised from 3 different aquifers: i) Na-Ca-SO_4^{2-}-HCO_3^- waters from the El Saladillo and El Reventón wells, belonging to the so-called La Ermita del Saladillo aquifer, which is the most extensive and deepest aquifer in the Gañuelas Mazarrón Tertiary basin; ii) Na-Ca-HCO_3^--SO_4^{2-} waters from the Gañuelas aquifer that show differences concerning to their SO_4^{2-} and Cl^- contents in

relation to waters from La Ermita del Saladillo aquifer, in spite of the two aquifers proximity; iii) Na-Mg-Cl^--HCO_3^- waters from the El Tiburón well; and iv) Na-Mg-Cl^--SO_4^{2-} waters from the Lorca well, both later water-wells belonging to the multilayered Totana aquifer. All these hydrofacies have very high salinity (EC); slightly acidity, with high DIC and free CO_2, and high calcite and aragonite saturation indexes. From an isotopic point of view, all of them have similar isotopic signatures ($\delta^{18}O$ and δ^2H), including $\delta^{13}C$ of DIC, and $\delta^{18}O$ and $\delta^{34}S$ of total dissolved sulphates. Isotopic signatures of waters ($\delta^{18}O$ and δ^2H) indicate a probable origin in relation to rainfalls from clouds originated in the Mediterranean Sea or in continental regions. The $\delta^{13}C$ values of DIC corroborate the main inorganic origin of C, with a low contribution of organic C. Furthermore, a contribution of CO_2 from terrestrial mantle, lower than 11%, can not be discarded. The $\delta^{18}O$ values of dissolved SO_4^{2-} indicate that only two hydrofacies are in isotopic equilibrium with water, whilst the remainders have been affected by cooling processes or contamination with shallow cold waters. Water from the Lorca well is extremely exceptional. The $\delta^{34}S$ signatures are, in general, supplied by the dissolution of the Messinian gypsum existing in the marly formation sealing the aquifer. Nevertheless, water from the Lorca well shows the lowest $\delta^{34}S$ values, indicating an origin related to gypsum formed at higher temperatures and to sulphur oxidation processes. Besides this, there are some important differences among these hydrofacies, which are: i) the higher temperatures of the El Saladillo, El Reventón and El Rincón waters than in El Tiburón and Lorca ones; ii) the redox conditions of the El Saladillo and El Reventón waters, clearly reduced, whilst the El Rincón, El Tiburón and Lorca waters are oxidised; iii) the Fe^{3+} contents, which are much higher in the El Saladillo, El Reventón and El Rincón waters than in the El Tiburón and Lorca ones; and iv) the variable Sr contents, being higher in the El Saladillo and El Tiburón waters (see Table 3).

Concerning carbonates, no clear relationship can be established with their corresponding parent-waters, since different hydrofacies can precipitate aragonite, calcite or a mixture of both. Thus, the El Saladillo and El Reventón waters precipitate aragonite, whereas El Rincón and Lorca precipitate calcite. However, El Tiburón water originates a mixture of both mineral phases, though in these samples diagenetic transformations were identified. As a consequence, it seems that no conclusive physicochemical parameters control the precipitation of one or another polymorph. Although this fact confirms the existing controversy in the specialised literature in

relation to the aragonite/calcite paradigm (see Jones and Renault, 2010), it is suggested that parent-waters from the El Saladillo and El Reventón wells have the most suitable physicochemical features for aragonite precipitation in this natural system. Furthermore, it is noticeable the disagreement between measured temperatures at the carbonate precipitation points and the inferred temperatures from the carbonate isotopic signature, except for sample SAL-1. In relation to the petrographic features, independently of the carbonate phase forming the precipitate, all samples have similar structural/textural characteristics, mainly induced by microbial/algae activity. Differences in petrographic patterns seem to reflect temporal variations in the travertines growth-rates, controlled by climatic factors. Geochemically, both parent-waters and resulting carbonates show chemical compositions indicating low dissolution, remobilization, transport and deposition of toxic elements, despite the acid character of all parent-waters. Only Fe is significant, but it can not be considered as a toxic element. It is mainly precipitated as Fe-oxy-hydroxides, which usually have high retention capacity, by adsorption, of heavy and more or less toxic elements, such as U, V, Zn, Mn and Cu. However, these Fe-oxy-hydroxides do not seem to contain significant amounts of these elements. Arsenic can only be considered as an exception in samples from the El Saladillo and El Reventón sites. The isotopic signature of both DIC and their corresponding carbonates could be used as good tracers for CO_2 leakages from an artificial deep geological storage of this greenhouse gas, despite the possible water/rock/gas interaction processes that could occur during its escape to the atmosphere. In this sense, $\delta^{13}C$ values of CO_2 from organic fuel combustion are very negative, around -30‰.

Finally, it can be stated that the fast precipitation of carbonates in this CO_2 storage and leakage natural analogue is mainly controlled by the rapid CO_2 degassing process and the subsequent sharp increase in the pH of their parent-waters. These precipitation processes can be favoured by the biological activity in some sites, as occur in Lorca and El Tiburón. In addition, the importance of this phenomenon mainly resides in its alarming character for CO_2 leakages either from any natural or artificial CO_2 storage, regardless of the carbonate phase formed. This rapid carbonate precipitation, either close or near to an artificial CO_2 storage, would be a strong warning of a possible leakage of the anthropogenic CO_2, indicating that the artificial storage is jeopardised.

All these findings lead to the conclusion that the study of natural analogues is a powerful tool to assess the long-term behaviour and safety of an artificial deep geological CO_2 storage. In this sense, the information obtained and the research

methodology followed can be applied to another similar geological site previously selected for a pilot or permanent storage of artificial CO_2. This application will be well framed in the general idea envisaging that: a comprehensive knowledge of any complex natural system will let us a better interaction with it, in order to predict its possible response.

6. REFERENCES

Anderson, T.F., Arthur, M.A., 1983. Stable isotopes of oxygen and carbon and their application to sedimentological and paleoenvironmental problems. Stable isotopes in sedimentary geology: Society of Economic Paleontologists and Mineralogists Short Course Notes 10, 1-151.

Arana, R., 1973. Investigaciones mineralógicas en Sierra Nevada (Cordilleras Béticas, España), Univ. Granada. Tesis Doctoral, 546 pp.

Arana, R., López-Aguayo, F., Ortega-Huertas, M., 1978. Wulfenita sedimentaria en el yacimiento de Montevives (Granada). Cuad. Geol. Univ. Granada 8-9, 75-82.

Back, W., Hanshaw, B.B., Plummer, L.N., Rahn, P.H., Rightmire, C.T., Rubin, M., 1983. Process and rate of dedolomitization: mass trasfer and 14C dating in a regional carbonate aquifer. Geol. Soc. Amer. Bull. 94, 1415-1429.

Ball, J.W., Nordstrom, D.K., 2001. User's manual for WATEQ4F, with revised thermodynamic data base and test cases for calculating speciation of major, trace, and redox elements in natural waters. U.S. Geological Survey Open-File Report, 91–183.

Barahona, E., 1974. Arcillas de ladrillería de la provincia de Granada. Evaluación de algunos ensayos en materias primas. Tesis Doctoral. Universidad de Granada, 398 pp.

Barragán, G., 1997. Algunos datos sobre la actividad hidrotermal pliocena al Oeste de Cuevas del Almanzora: Encuadre geológico y cronológico de las manifestaciones magmáticas e hidrotermales de la depresión de Vera (Provincia de Almería). In: L. García-Rossell, L., Navarro, A. (Eds.), Recursos Naturales y Medio Ambiente en el Sudeste Peninsular, Instituto de Estudios Almerienses, pp. 205-223.

Berner, R.A., 1997. The rise of plants and their effect on weathering and atmospheric CO_2. Science 276, 544-546.

Böhm, F., Joachimski, M.M., Dullo, W.C., Eisenhauer, A., Lehnert, H., Reitner, J., Wörheide, G., 2000. Oxygen isotope fractionation in marine aragonite of coralline sponges. Geochim. Cosmochim. Acta 64, 1695-1703.

Cerling, T.E., 1984. The stable isotopic composition of modern sil carbonate and its relationship to climate. Earth Planet. Sc. Lett. 71, 229-240.

Cerling, T.E., 1991. Carbon dioxide in the atmosphere: evidence from Cenozoic and Mesozoic paleosols. Am. J. Sci. 291, 377-400.

Cerón, J.C., Martín-Vallejo, M., García-Rossell, L., 1998. Geoquímica de las aguas termales con CO_2 del SE de las Cordilleras Béticas. Estudios Geol. 54, 199-207.

Cerón, J.C., Martín-Vallejo, M., García-Rossell, L., 2000. CO_2-rich thermomineral groundwater in the Betic Cordilleras, southeastern Spain: Genesis and tectonic implications. Hydrogeol. J. 8, 209-217.

Chafetz, H.S., Folk, R.L., 1984. Travertines: depositional morphology and the bacterially constructed constituents. J. Sediment. Petrol. 54, 289-316.

Cohn, M., Urey, H.C., 1938. Oxygen exchange reactions of organic compounds and water. J. Am. Chem. Soc. 60, 679-687.

Craig, H., 1961. Isotopic variations in meteoric waters. Science 133, 1702-1703.

Craig, H., 1965. The measurement of oxygen isotope paleotemperatures. In: Tongiorgi, E. (Ed.), Stable Isotopes in Oceanographic Studies and Paleotemperatures. Spoleto, Consiglio Nazionale delle Ricerche, Laboratorio di Geologica Nucleare, Pisa, pp. 161–182.

Deines, P., 1980. The isotopic composition of reduced organic carbon. In: Fritz P., Fontes J.Ch. (Eds.), Handbook of Environmental Isotope Geochemistry, Vol. 1. Elsevier, New York, pp. 329-406.

Delgado, A., 1994. Estudio isotópico de los procesos diagenéticos e hidrotermales relacionados con la génesis de bentonitas (Cabo de Gata, Almería), Universidad de Granada, 413 pp.

Delgado, A., Reyes, E., 2004. Isótopos estables como indicadores paleoclimáticos y paleohidrológicos en medios continentales. Seminarios de la Sociedad Española de Mineralogía. Geoquímica Isotópica Aplicada al Medioambiente 1, 37-53.

Deutsch, W.J., Jenne, E.A., Y Krupka, K.M., 1982. Solubility equilibria in basalt aquifers: the Columbia Plateau, Eastern Washington, USA. Chem. Geol. 36, 15-34.

Epstein, S., Buchsbaum, R., Lowenstam, H., 1953. Carbonate-water isotopic temperature scale. Geol. Soc. Am. Bull. 62, 417-425.

Epstein, S.Y., Mayeda, T.K., 1953. Variation of the $^{18}O/^{16}O$ ratio in natural waters. Geochim. Cosmochim. Acta 4, 213–224.

Farmer, J.D., Des Marais, D.J., 1994. Biological versus inorganic processes in stromatolite morphogenesis: Observations from mineralizing sedimentary systems. In: Stal, L.J., Caumette, P., (Eds.), Microbial Mats: Structure, Development, and Environmental Significance: NATO ASI Series in Ecological Sciences, v. G35, Berlin, Springer-Verlag, pp. 61-68.

Fernández Rubio, R., Eraso, A., Ortega Huertas, M., Arana, R., Rojas, E., 1975. Estudio de la sima termal de Las Fumarolas (Montevives, Granada, España). Ann. Spéléol. 30, 287-302.

Folk, R.L., 1974. The natural history of crystalline calcium carbonate: effect of magnesium content and salinity. J. Sediment Petrol. 44, 40-53.

Folk, R.L., 1994. Interaction between bacteria, nannobacteria and mineral precipitation in hot springs of central Italy. Géogr. Phys. Quatern. 48, 233-246.

Folk, R.L., Chafetz, H.S., Tiezzi, A., 1985. Bizarre forms of depositional and diagenetic calcite in hot-spring travertines, central Italy. In: Schneidermann, N., Harris, M. (Eds), Carbonate Cements. SEPM Special Publication 36, pp. 349-369.

Ford, T.D., Pedley, H.M., 1996. A review of tufa and travertine deposits of the world. Earth-Sci. Rev. 41, 117-175.

Fouke, B.W., Farmer, J.D., Des Marais, D.J., Pratt, L., Sturchio, N.C., Burns, P.C., Discipulo, M.K., 2000. Depositional facies and aqueous–solid geochemistry of travertine depositing hot springs (Angel Terrace, Mammoth Hot Springs, Yellowstone National Park, U.S.A.). J. Sediment. Res. 70, 265–285.

Freytet, P., Verecchia, E.P., 1998. Freshwater organisms that build stromatolites: a synopsis of biocrystallization by prokaryotic and eukaryotic algae. Sedimentology 45, 535-563.

Friedman, I., 1970. Some investigations of the deposition of travertine from hot springs: I. The isotope chemistry of a travertine-depositing spring. Geochim. Cosmochim. Acta 34, 1303-1315.

Friedman, I., O'Neil, J.R., 1977. Compilation of stable isotope fractionation factors of geochemical interest. Data of Geochemistry. U. S. Geol. Surv. Prof. Pap. 440-KK, 6th ed.

Frisia, S., Borsato, A., Fairchild, I.J., McDermott, F., 2000. Calcite fabrics, growth mechanisms, and environments of formation in speleothems from the Italian Alps and Southwestern Ireland. J. Sediment. Res. 70, 1183-1196.

García-Guinea, J., Morales, S., Delgado, A., Recio, C., Calaforra, J.M., 2002. Formation of gigantic gypsum crystals. Geol. Soc. J. 159, 347–350.

Gat, J.R., Carmi, I., 1970. Evolution in the isotopic composition of atmospheric waters in the Mediterranean Sea area. J. Geophys. Res. 75, 3039–3048.

Gehre, M., Geilmann, H., Richter, J., Werner, R.A., Brand, W.A., 2004. Continuous flow $^{2}H/^{1}H$ and $^{18}O/^{16}O$ analysis of water samples with dual inlet precision. Rapid Communications in Mass Spectrometry, 18, 2650.

Gómez-Pugnaire, M.T., Torres-Ruiz, J., Martínez Martínez, J.M. 1981. Escapolita en rocas de las series Permo-Triásicas del Complejo Nevado-Filábride (Cordilleras Béticas). Origen. Bol. Soc. Esp. Min., IV, 37-46.

González, P.J., Tiampo, K.F., Palano, M., Cannavó, F., Fernández, J., 2012. The 2011 Lorca earthquake slip distribution controlled by groundwater crustal unloading. Nature Geoscience, DOI: 10.1038/NGEO1610.

Grossman, E.L., Ku, T-L., 1986. Oxygen and carbon isotope fractionation in biogenic aragonite: Temperature effects. Chem. Geol. 59, 59-74.

Guo, L., Andrews, J., Riding, R., Dennis, P., Dresser, Q., 1996. Possible microbial effects on stable carbon isotopes in hot spring travertine. J. Sediment. Res. 66, 468-473.

Guo, L., Riding, R., 1998. Hot-spring travertine facies and sequences, Late Pleistocene, Rapolano Terme, Italy. Sedimentology 45, 163-180.

Guo, L., Riding, R. 1999. Rapid facies changes in Holocene fissure ridge hot spring travertines, Rapolano Terme, Italy. Sedimentology 46, 1145-1158.

Herrero, M.J., Escavy, M.J., 2010. Economic Aspects of Continental Carbonates and Carbonates Transformed under Continental Conditions. In: Carbonates in Continental Settings: Geochemistry, Diagenesis and Applications. Developments in Sedimentology 66, 275-296.

IGME, 1974. Mazarrón (Hoja 976). Ministerio de Industria, Madrid, 26 pp.

IGME, 1979. La problemática de las aguas en el término municipal de Totana (Murcia), 26 pp.

IGME, 1981. Los recursos hídricos subterráneos de la Comarca Mazarrón-Águilas. Situación actual y perspectivas futuras, 4 tomos.

IGME, 1985. Investigación de las posibilidades de existencia de energía geotérmica en la comarca de Mazarrón-Águilas. ADARO-IGME.

IGME, 2008. INAQUAS. Aplicación informática y manual.

Jones, B., Renault, R.W., 2010. Calcareous spring deposits in continental settings. In: Carbonate in continental settings: Geochemistry, diagenesis and applications. Developments in Sedimentology 66, 177-215.

Kim, S.T., O´Neil, J.R., 1997. Equilibrium and nonequilibrium oxygen isotope effects in synthetic carbonates. Geochim. Cosmochim. Acta 61, 3461-3475.

Kim, S.T., O´Neil, J.R., Hillarie-Marcel, C., Mucci, A., 2007. Oxygen isotope fractionation between synthetic aragonite and water: Influence of temperature and Mg^{2+} concentration. Geochim. Cosmochim. Acta 71, 4704-4715.

Kitano, Y., 1962. A study of the polymorphic formation of calcium carbonate in therma springs with an emphasis on the effect of temperature. Bull. Chem. Soc. Jpn. 35, 1980-1985.

Kitano, Y., Hood, D.W., 1965. The influence of organic matter on the polymorphic crystallization of calcium carbonate. Geochim. Cosmochim. Acta 29, 29-41.

Klug, H.P., Alexander, L.E., 1974. X-Ray diffraction procedures. J. Willey, 2nd edition, New York, 966 pp.

Kusakabe, M., Robinson, B.W., 1977. Oxygen and sulphur isotope equilibria in $BaSO_4$-HSO_4^--H_2O system from 110 to 350 degrees-C and applications. Geochim.Cosmochim. Acta 41, 1033-1040.

Longinelli, A. 1979. Isotope geochemistry of some Messinian evaporites; paleoenvironmental implications. Palaeogeogr. Palaeoclimatol. Palaeoecol. 29, 95–123.

Martín Pozas, J.M., 1968. Análisis cuantitativo de los filosilicatos de la arcilla por difracción de rayos X. Tesis Doctoral, Universidad de Granada, 194 pp.

Martín, J., Ortega-Huertas, M., Torres-Ruiz, J., 1984. Genesis and evolution of strontium deposits of the Granada basin (Southeastern Spain) Evidence of diagenetic replacement of a stromatolite belt. Sediment. Geol. 39, 281-298.
McCrea, J.M., 1950. On the isotopic chemistry of carbonates and a paleotemperature scale. J. Chem. Phys. 18, 849-857.

Meyer, H.J., 1984. The influence of impurities on the growth rate of calcite. J. Cryst. Growth 66, 639-646.

Moore, G.W., 1956. Aragonite speleothems as indicators of paleotemperature. Am. J. Sci. 254, 746-753.

Navarro, A., Fernández-Uría, A., Doblas, J.G., 1993. Las aguas subterráneas en España: Estudio de síntesis, Instituto Tecnológico Geominero de España, Madrid, Spain.

Nemeth, K., 1963. Photometric determination of sulphate in soil extracts. Z. PflErnahr. Dung. 103, 193–196.

Nisi, B., Vaselli, O., Tassi, F., Gimeno, M.J., Acero, P., Poreda, R.J., Rodrigo-Naharro, J., Delgado, A., Pérez del Villar, L., 2010a. Effects of deep saline CO_2-rich waters in the shallow aquifers from the Mazarrón-Gañuelas Tertiary basin (central-southern Spain). Proceedings of the 85º Congresso Nazionale; 2010 Sep 6-8, Pisa, Italy. Società Geologica Italiana; 2010. Rend. Soc. Geol. It., 11, 186-187 (on line).

Nisi, B., Vaselli, O., Tassi, F., Gimeno, M.J., Acero, P., Poreda, R.J., Rodrigo-Naharro, J., Delgado, A., Pérez del Villar, L., 2010b. Water deterioration of the Mazarrón-Gañuelas aquifer (SE Spain) by deep-seated CO_2 saline-waters as evidenced by geochemical and isotopic investigation. Proceedings of the 89th SIMP Meeting; 2010 Sep 13-15, Ferrara, Italy. Societá Italiana di Mineralogia e Petrologia; 2010, S2.2-O3.

Nordstrom, D.K., Ball, J.W., 1989. Mineral saturation states in natural waters and their sensitivity to thermodynamic and analytic errors. Sci. Geol. Bull. 42, 269-280.

Ortega Huertas, M., 1973. Estudio mineralógico del yacimiento de estroncio de Montevives (Granada). Dpto. de Cristalografía y Mineralogía, Univ. de Granada. Tesis de Licenciatura, 202 pp.

Ortega Huertas, M., Arana, R., Rodríguez Gallego, M., 1973. Minerales de la arcilla en el yacimiento de Montavives (Granada). Estud. Geol. 29, 451-455.

Ortega Huertas, M., Arana, R., Rodríguez Gallego, M., 1974. Observaciones mineralógicas y geoquímicas sobre el yacimiento de estroncio de Montevives (Granada). Cuad. Geol. Univ. de Granada 5, 5-19.

Owen, R., Kennedy, H., Richardson, C., 2002. Experimental investigation into partitioning of stable isotopes between scallop (*Pecten maximus*) shell calcite and sea water. Palaeogeogr. Palaeocl. Palaeoecol. 185, 163-174.

Parkhurst, D.L., Appelo, C.A.J., 1999. User's Guide to PHREEQC (Version 2), a computer program for speciation, batch-reaction, one-dimensional transport, and inverse geochemical calculations. Water Resources Research Investigations Report 99-4259, 312 pp.

Patterson, W.P., Smith, G. R., Lohmann, K.C., 1993. Continental paleothermometry and seasonality using the isotopic composition of aragonitic otoliths of freshwater fishes. Geophy. Monogr. 78, 191-202.

Pentecost, A., 1990. The formation of travertine shrubs: Mammoth Hot Springs, Wyoming. Geol. Mag. 127, 159-168.

Pentecost, A., 2005. Travertine. Springer, Berlin, 445 pp.

Pentecost, A., Viles, H., 1994. A review and reassessment of travertine classification. Géogr. Phys. Quatern. 48, 305-314.

Pérez, N.M., Nakai, S., Wakita, H., Beltrán, A., Redondo, R., 1996. Preliminary results on $^{3}He/^{4}He$ isotopic ratios in terrestrial fluids from Iberian Peninsula: seismotectonic and neotectonic implications. Geogaceta 20, 830-833.

Pérez del Villar et al., 2009. Memoria Científico-Técnica del periodo 2008-2009 del PSE-120000-2008-6 (PSS-120000-2008-31). Línea de Análogos Naturales: "Resultados preliminares del estudio de los análogos naturales estudiados en: la región de La Selva (Girona), Valle del Alto Guadalentín (Murcia-Almería), Alicún de las Torres (Granada), Alhama de Aragón-Járaba (Zaragoza) y Castilla León, 550 pp.

Plummer, L., Busenberg, N.E., 1982. The solubilities of calcite, aragonite and vaterite in $CO_2 – H_2O$ solutions between 0 and 90 °C, and an evaluation of the aqueous model for the system $CaCO_3 – CO_2 – H_2O$. Geochim. Geochim. Acta 46, 1011–1040.

Prado-Pérez, A.J., 2011. El Sistema Termal de Alicún de las Torres (Granada) como Análogo Natural de Escape de CO_2 en forma de DIC: Implicaciones Paleoclimáticas y como Sumidero de CO_2. Universidad Complutense de Madrid, 411 pp.

Prado-Pérez, A.J., Pérez del Villar, L. 2011. Dedolomitization as an analogue process for assessing the long-term behaviour of a CO_2 deep geological storage: The Alicún de las Torres thermal system (Betic Cordillera, Spain). Chem. Geol. 289, 98-113.

Prado-Pérez, A.J., Delgado Huertas, A., Crespo, M.T., Martín Sánchez, A., Pérez del Villar, L., 2013. Late Pleistocene and Holocene paleoclimatic and palaeoenvironmental reconstruction at middle geographical latitude. An approach based on the isotopic record from a travertine formation in the Guadix-Baza basin (Spain). Geol. Mag. (on line).

Reyes, E., Pérez del Villar, L., Delgado, A., Cortecci, G., Núñez, R., Pelayo, M., Cózar, J., 1998. Carbonatation processes at the El Berrocal analogue granitic system (Spain): mineralogical and isotopic study. Chem. Geol. 150, 293-315.

Rodrigo-Naharro, J., Nisi, B., Vaselli, O., Lelli, M., Saldaña, R., Clemente-Jul, C., Pérez del Villar, L., 2013. Diffuse soil CO_2 flux to assess the reliability of CO_2 storage in the Mazarrón-Gañuelas Tertiary Basin (Spain). Fuel (in press).

Rodrigo-Naharro, J., Nisi, B., Vaselli, O., Quindós, L.S., Pérez del Villar, L., 2012. Measurements and relationships between CO_2 and ^{222}Rn in a natural analogue for CO_2 storage and leakage: the Mazarrón Tertiary Basin (Murcia, Spain). Geo-Temas 13, 1978-1981.

Rodrigo-Naharro, J., Vaselli, O., Tassi, F., Clemente-Jul, C., Pérez del Villar, L. 2011. Effects on the shallow aquifers by CO_2 leakages in a tertiary basin (province of Murcia, Spain). Fifth International Conference on Clean Coal Technologies CCT2011, Zaragoza (Spain).

Rodríguez-Estrella, T. 2006. Hidrogeología de la Región de Murcia. In: Conesa, C. (Ed.), El medio físico de la Región de Murcia, Universidad de Murcia, pp. 143-181.

Romanek, C.S., Grossman, E.L., Morse, J.W., 1992. Carbon isotopic fractionation in synthetic aragonite and calcite: Effects of temperature and precipitation rate. Geochim. Cosmochim. Acta 56, 419-430.

Salata, G.G., Roelke, L.A., Cifuentes L.A., 2000. A rapid and precise method for measuring stable carbon isotope ratios of dissolved inorganic carbon. Mar. Chem. 69, 153–161.

Sanz de Galdeano, C., Ortega Huertas, M., Arana, R., 1976. Nuevo yacimiento de celestina en la depresión de Granada. Estudio geológico y mineralógico. Estud. Geol. 32, 435-442.

Sanz de Galdeano, C., López-Casado, C., Delgado, J., Peinado, M.A., 1995. Shallow seismicity and active faults in the Betic Cordillera. A preliminary approach to seismic sources associated with specific faults. Tectonophysics 248, 293-302.

Schultz, L.G., 1964. Quantitative interpretation of mineralogical composition from X-ray and chemical data for the Pierre Shale. U. S. Geol. Survey Prof. Pap., 391-C, 31 pp.

Shackleton, N.J., Opdyke, N.D., 1973. Oxygen isotope and palaeomagnetic stratigraphy of equatorial Pacific core V28-238: Oxygen isotope temperatures and ice volumes on a 10^5 and 10^6 year scale. Quat. Res. 3, 39-55.

Sharp, Z.D., Atudorei, V., Durakiewicz, T., 2001. A rapid method for determination of hydrogen and oxygen isotope ratios from water and hydrous minerals. Chem. Geol. 178, 197-210.

Tena, J.M., Auqué, L.F., Gimeno, M.J., Femández, J., Mandado, J., 1990. El equilibrio cuarzo/solución de 0 a 100° C. Variaciones en el cálculo de *K* según los calibrados geotermométricos y las funciones de *T* utilizadas en programas de modelización geoquímica. Estud. Geol. 46, 15-24.

Thorrold, S.R., Campana, S.E., Jones, C.M., Swart, P.K., 1997. Factors determining $\delta^{13}C$ and $\delta^{18}O$ fractionation in aragonitic otoliths of marine fish. Geochim. Cosmochim. Acta 61, 2909-2919.

Turi, B., 1986. Stable isotope geochemistry of travertines. In: Fritz, P., Fontes, J.Ch. (Eds.), Handbook of Environmental Isotope Geochemistry, 2, The terrestrial environment, Elsevier, pp. 207-238.

Valero-Garcés, B.L., Delgado-Huertas, A., Ratto, N., Navas, A., Machin, J., 1999. Large ^{13}C enrichment in primary carbonates from Andean Altiplano lakes, Northwest Argentina. Earth Planet. Sc. Lett. 171, 253-266.

Vaselli, O., Nisi, B., Tassi, F., Rodrigo-Naharro, J., Pérez Del Villar, L., 2010. Diffuse soil CO_2 flux and water and dissolved gas geochemistry in the Gañuelas-Mazarrón area (Guadalentin Valley). Final Report, 66 pp.

Viles, H.A., Pentecost, A., 2007. Tufa and travertine. In: Nash, D.J., McLaren, S.J. (Eds.), Geochemical Sediments and Landscapes, Wiley-Blackwell, Oxford, pp. 173-199.

White, R.M.P., Dennis, P.F., Atkinson, T.C., 1999. Experimental calibration and field investigation of the oxygen isotopic fractionation between biogenic aragonite and water. Rapid Commun. Mass Spectrom. Rev. 13, 1242-1247.

Zhou, G.T., Zheng, Y.F., 2003. An experimental study of oxygen isotope fractionation between inorganically precipitated aragonite and water at low temperatures. Geochim. Cosmochim. Acta 67, 387-399.

1135-9420